Synthesis, Conformational Analysis, and Cytotoxicity of Conformationally Constrained Aplidine and Tamandarin A Analogues Incorporating a Spirolactam β-Turn Mimetic

Marta Gutiérrez-Rodríguez,[§] Mercedes Martín-Martínez,[§] M. Teresa García-López,[§] Rosario Herranz,*,[§] Félix Cuevas,[‡] Concepción Polanco,[‡] Ignacio Rodríguez-Campos,[‡] Ignacio Manzanares,[‡] Francisco Cárdenas,[#] Miguel Feliz,[#] Paul Lloyd-Williams,*,[†] and Ernest Giralt[†,‖]

Instituto de Química Médica (CSIC), Juan de la Cierva 3, E-28006 Madrid, Spain, Pharma Mar, S.A., Polígono Industrial La Mina, Avda. de los Reyes 1, E-28770 Colmenar Viejo, Madrid, Spain, Unidad de RMN de Alto Campo, SCT, Universidad de Barcelona, Josep Samitier 1, E-08028 Barcelona, Spain, Departamento de Química Orgánica, Universidad de Barcelona, Martí i Franquès 1-11, E-08028 Barcelona, Spain, and IRBB-Parque Científico de Barcelona, Josep Samitier 1, E-08028 Barcelona, Spain

With the aim of studying the contribution of the β II turn conformation at the side chain of didemnins to the bioactive conformation responsible for their antitumoral activity, conformationally restricted analogues of aplidine and tamandarin A, where the side chain dipeptide Pro[8]-*N*-Me-D-Leu[7] is replaced with the spirolactam β II turn mimetic (5*R*)-7-[(1*R*)-1-carbonyl-3-methylbutyl]-6-oxo-1,7-diazaspiro[4.4]nonane, were prepared. Additionally, restricted analogues, where the aplidine (pyruvyl[9]) or tamandarin A [(*S*)-Lac[9]] acyl groups are replaced with the isobutyryl, Boc, and 2-methylacryloyl groups, were also prepared. These structural modifications were detrimental to cytotoxic activity, leading to a decrease of 1−2 orders of magnitude with respect to that exhibited by aplidine and tamandarin A. The conformational analysis of one of these spirolactam aplidine analogues, by NMR and molecular modeling methods, showed that the conformational restriction caused by the spirolactam does not produce significant changes in the overall conformation of aplidine, apart from preferentially stabilizing the trans rotamer at the pyruvyl[9]−spirolactam amide bond, whereas in aplidine both cis and trans rotamers at the pyruvyl[9]−Pro[8] amide bond are more or less equally stabilized. These results seem to indicate a preference for the cis form at that amide bond in the bioactive conformation of aplidine. The significant influence of this cis/trans isomerism upon the cytotoxicity suggests a possible participation of a peptidylprolyl cis/trans isomerase in the mechanism of action of aplidine.

Introduction

The didemnins are a family of macrocyclic depsipeptides, isolated from several tunicates, which exhibit a wide variety of biological activities, including antitumor,[1,2] antiviral,[2] and inmunosupresive properties.[2,3] These depsipeptides share a common 23-membered macrocycle made up of six subunits [(3*S*,4*R*,5*S*)-isostatine (Ist[1]), (2*S*,4*S*)-3-oxo-4-hydroxy-2,5-dimethylhexanoic acid (Hip[2]), Leu[3], Pro[4], [N,O-(Me)₂-Tyr[5]], and Thr[6]] and differ in the side chain attached to the threonine NH, through a *N*-Me-D-leucine residue. Didemnin B (Figure 1, **1**), isolated in 1981 from the Caribbean tunicate *Trididemnum solidum*,[4] and aplidine (**2**, dehydrodidemnin B), isolated in 1990 from the Mediterranean tunicate *Aplidium albicans*,[5] stand out because of their potent antitumoral activity. Didemnin B was the first marine natural product to enter human anticancer trials, but these had to be discontinued during
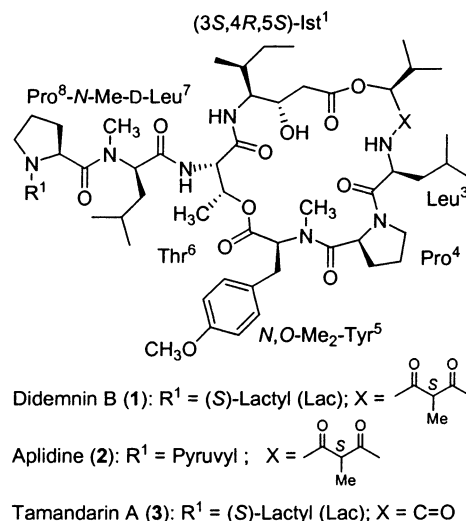

Figure 1. Most relevant didemnins and tamandarin A.

phase II tests because of its neuromuscular and cardiotoxicity.[1,2] Aplidine showed higher antitumoral potencies and lower toxicity in preclinical and phase I clinical studies.[1,2,6−9] This better therapeutic profile has facilitated its recent entry into phase II clinical trials.

Although the mechanism of action of aplidine is not completely elucidated, it is known that it exerts anti-

* To whom correspondence should be addressed. For R.H.: phone, +34 91 5622900; fax, +34 91 5644853; e-mail, rosario@iqm.csic.es. For P.L.-W.: phone, +34 93 4021260; fax, +34 93 3397878; e-mail, lloyd@qo.ub.es.
§ Instituto de Química Médica (CSIC).
‡ Pharma Mar, S.A.
# Unidad de RMN de Alto Campo, SCT, Universidad de Barcelona.
† Departamento de Química Orgánica, Universidad de Barcelona.
‖ IRBB-Parque Científico de Barcelona.

proliferative effects through the inhibition of protein synthesis and ornithine decarboxylase activity[10–12] and by induction of arrest and blockade of the G_1 and G_2 cell cycle phases, respectively.[13] Additionally, aplidine inhibits vascular endothelial growth factor (VEGF) secretion and decreases the expression of its receptor VEGFR-1 in human leukemia cells MOLT-4.[14] Also, in leukemic cells, aplidine is an extremely potent and rapid apoptotic inductor via mitochondrial-mediated apoptotic signaling routes[15] and through activation of several intracellular signaling kinases.[16]

Structure−activity relationship studies on didemnins have shown the importance of the integrity of the macrocyclic skeleton.[2,17–19] However, two analogues, tamandarins A (Figure 1, **3**) and B, have recently been isolated from a Brazilian ascidian of the family Didemnidae,[20] which were reported to be somewhat more potent in vitro than didemnin B.[20,21] These analogues have a hydroxyisovaleric acid (Hiv²) unit in the macrocyclic core instead of the hydroxyisovalerylpropionic acid (Hip²) unit of the didemnins. With regard to the side chain, it is difficult to establish precise structure−activity relationships from the described data, but it is important for activity, since the macrocycle hydrochloride was completely inactive[22] and simple *N*-acyl derivatives at the threonine NH retained very little antitumor activity.[19] The (*N*-Me-D-Leu⁷) residue (both the *N*-methyl group and the D configuration must be present) is essential for antitumoral activity.[19,23]

X-ray diffraction analysis of the didemnin B (**1**) crystal structure showed that its macrocycle was twisted and puckered with a shape that was described as a "bent figure eight".[24] This conformation was stabilized by three intramolecular hydrogen bonds: a strong hydrogen bond between the (Leu³) carbonyl and the (Ist¹) amino group, forcing the adoption of the figure eight shape, which is stabilized by another hydrogen bond between the (*N*-Me-D-Leu⁷) carbonyl and the (Leu³) amino group, and the third bond from the lactic (Lac⁹) carbonyl to the (Thr⁶) amino group. This third hydrogen bond fixes the linear side chain folded back toward the macrocycle into a β II turn conformation. Two previous conformational studies on didemnin B, using computational methods and solution NMR in deuterated DMSO-d_6[25] and CDCl₃,[26] showed the presence of a preferred conformation, which overall was quite similar to the crystal structure previously determined by X-ray crystallography. The conformational comparison of tamandarin A (**3**) with didemnin B, using various NMR methods, showed that in fact the conformations of both congeners in solution are strikingly similar and have the same hydrogen bond network.[20] On the other hand, recent conformational studies on aplidine (**2**), also in comparison with didemnin B, have shown the presence of two slowly exchanging preferred conformers due to the restricted rotation about the amide bond between the (pyruvyl⁹) and (Pro⁸) side chain residues.[27,28] These conformations correspond to the cis and trans isomers at that amide bond, and both are stabilized by a hydrogen bond between the (Thr⁶) NH and the pyruvylcarboxamide C=O in the trans isomer or the (pyruvyl⁹) keto group in the cis isomer (Figure 2). In CDCl₃ the cis/trans ratio was (~1:1),[27] while in DMSO there was a (6:4) preference for the cis conformer.[28] However,
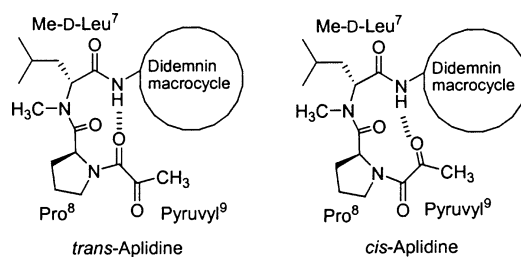

Figure 2. Aplidine side chain preferred conformations.

despite the localized differences between these two conformers, both present similar hydrogen-bonding patterns, and their overall conformations are alike and broadly similar to that of didemnin B.

The fact that biological activities of the didemnins are strongly dependent on the structure of the linear side chain, along with its preference for adopting a β II turn conformation, has led to speculation that this conformational feature may be a determining element of biological activity. Thus, some authors have suggested that the side chain does not directly participate in the binding of the didemnins to their receptors but that it may stabilize the bioactive conformation of the macrocycle through the formation of a β turn,[29] while others have suggested that the presence of this turn is not essential for activity.[2,30] With the aim of shedding light on this issue and contributing to the study of the bioactive conformation of the didemnins, as a first step toward the design of aplidine peptidomimetics, we synthesized aplidine and tamandarin A analogues **4a** and **5a** (Figure 3), where the Pro⁸-*N*-Me-D-Leu⁷ dipeptide of the side chain was replaced by a [4.4]spirolactam β II turn mimetic. This replacement fixes the dipeptide conformation with an additional methylene bridge and allows the essential side chain and configuration of the (D-Leu⁷) residue at the *i + 2* position of the β turn to be retained. Furthermore, according to the described data for this type of β turn mimetic, it would fix the dipeptide backbone ϕ_8, ψ_8, ϕ_7, and ψ_7 torsion angles into values (−50.9°, 128.7°, 91.1°, and −5.4°) very close to those of an ideal type II β turn[31] and also near those observed in the crystal structure of didemnin B[24] and those calculated for aplidine.[27] On the other hand, because the replacement of the [(*S*)-Lac⁹] group of didemnin B by short-chain aliphatic acyl groups did not significantly affect its antitumor activity,[18,30] we also prepared analogues **4b,c** and **5b−d**, where the (pyruvyl⁹) moiety (**a**) was replaced by the isobutyryl (**b**), Boc (**c**), and 2-methylacryloyl (**d**) groups. The cytotoxicities of these didemnin analogues were determined in human lung (A549) and colon (HT-29) carcinoma cell lines. Finally, with the aim of establishing conformation−cytotoxicity relationships, the effect of the local conformational constraint on the global conformation was studied in the aplidine analogue **4a**, in comparison with aplidine and didemnin B, by using NMR and molecular modeling methods. This conformational analysis required the parallel analysis of the spirolactam derivative **6a** (Figure 3) as a simple model of the side chain dipeptide.

Results and Discussion

Synthesis. The preparation of the aplidine and tamandarin analogues **4** and **5** required the coupling of their respective macrocycles to the appropriate [4.4]-
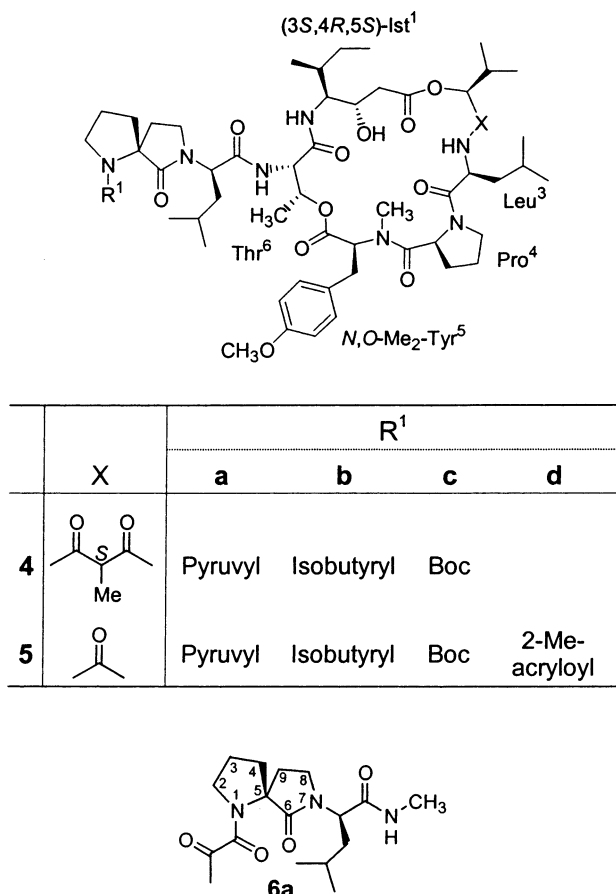
Figure 3. Spirolactam analogues of aplidine (**4**), tamandarin A (**5**), and the dipeptide pyruvyl-Pro-*N*-Me-D-Leu-NHMe (**6a**).

spirolactam pseudodipeptide derivatives **9a–d**, which were obtained from the spirolactam analogue of H-Pro-*N*-Me-D-Leu-OBn **7**[32] by acylation and subsequent C deprotection, as shown in Scheme 1. Attempts to introduce the pyruvyl group as described for the synthesis of aplidine[33] by coupling the trifluoroacetate **7** with pyruvic acid using DCC/HOBt as activating agents were unsuccessful. This coupling required the use of HOAt/HATU as activating reagents and DIEA as base, or alternatively, it was also carried out using pyruvyl chloride as acylating agent, which had been freshly prepared from pyruvic acid and dichloromethyl methyl ether.[34] In both cases the yield of the *N*-pyruvyl derivative **8a** was not higher than 50%. Catalytic hydrogenolysis of this compound in the presence of 10% Pd(C) led quantitatively to the corresponding C-deprotected spiropseudodipeptide **9a**. Activation of this acid with BOP, followed by treatment with methylamine hydrochloride, led to the *N*-methylcarboxamide **6a**. The isoburyryl and 2-methylacryloyl derivatives **8b** and **8d** were obtained by reaction of trifluoroacetate **7** with the isobutyryl and 2-methylacryloyl chlorides, respectively, in the presence of TEA and catalytic amounts of 4-(dimethylamino)pyridine (DMAP). The C deprotection of the isobutyryl derivative **8b** was also carried out by catalytic hydrogenolysis. However, in the case of the 2-methylacryloyl derivative **8d**, hydrogenation, even using a Lindlar catalyst, led to the simultaneous reduction of the double bond and C deprotection, furnishing **9b**. Consequently, in this case the C deprotection was carried out by saponification to give **9d**. The reaction of
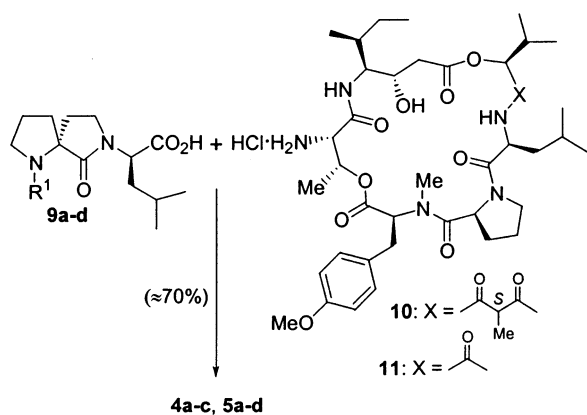
Scheme 1[a]
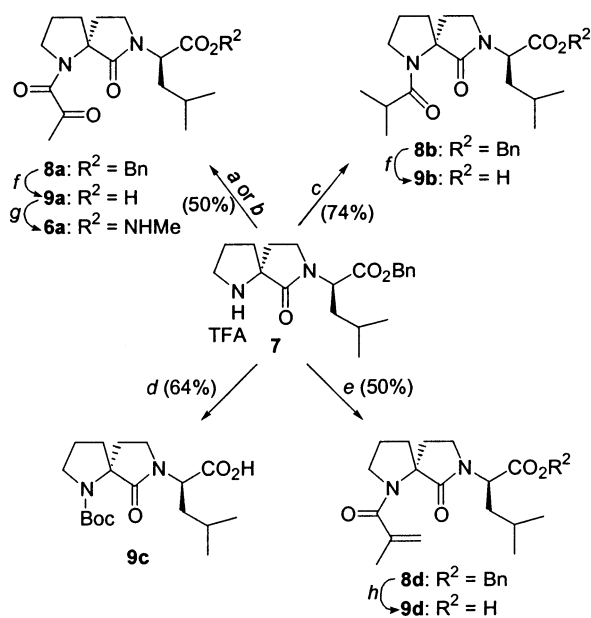
[a] Reagents: (a) CH$_3$COCO$_2$H, HATU, HOAt, NMM, CH$_2$Cl$_2$; (b) CH$_3$COCOCl, TEA, DMAP, CH$_2$Cl$_2$; (c) (CH$_3$)$_2$CHCOCl, TEA, DMAP, CH$_2$Cl$_2$; (d) Boc$_2$O, (CH$_3$)$_4$NOH·H$_2$O, CH$_3$CN; (e) CH$_2$=C-(CH$_3$)–COCl, TEA, DMAP, CH$_2$Cl$_2$; (f) H$_2$, Pd(C), MeOH; (g) MeNH$_2$·HCl, BOP, NMM, CH$_2$Cl$_2$; (h) 1 N NaOH, MeOH.

the trifluoroacetate **7** with di(*tert*-butyl) dicarbonate in dry acetonitrile, using tetramethylammonium hydroxide as base,[35] led directly to the *N*-Boc-acylated and C-deprotected pseudodipeptide **9c**.

The ^{1}H and ^{13}C NMR spectra of the *N*-pyruvyl derivatives **8a** and **9a** and the *N*-Boc derivative **9c** in CDCl$_3$ showed the presence of two conformations at the carboxamide bond in a 2:1 ratio. As in the case of aplidine,[27] in the pyruvic acid derivative **8a** these slowly exchanging conformational isomers were also observed by TLC and HPLC. The assignment of these conformations was based on a comparison of the chemical shifts for the C$_2$ and C$_5$ carbons of both conformations in each compound, as is usually applied for Xaa–proline amide bond isomers.[36–38] Thus, in the *N*-pyruvyl derivatives **8a** and **9a** the major conformer was assigned as trans because its C$_2$ signal appeared downfield (48.91 ppm for **8a** and 49.30 ppm for **9a**) from that of the minor isomer (47.72 and 48.03 ppm, respectively) while its C$_5$ signal appeared upfield (66.82 and 69.11 ppm) to that of the cis isomer (67.82 and 69.11 ppm). However, by application of the same criteria, in the *N*-Boc derivative **9c** the major conformation was assigned as cis. The high percentage of the cis form in this derivative (66%) is in agreement with the known preference of urethane *N*-protected amino acids to adopt this conformation, as exemplified by Boc-proline.[39] In the isobutyryl derivatives **8b** and **9b** and the 2-methylacryloyl derivatives **8d** and **9d**, only one preferred conformation was observed, which was assigned as trans for the last two compounds, based on the NOE effects observed in their 1D NOESY spectra between the (acryloyl) CH$_2$ protons and the 2-H spirolactam protons. This experiment could not be used for determining the conformation of the isobutyryl–Pro amide bond in compounds **8b** and **9b** because the signals corresponding to their 2-H protons overlapped with those of their 8-H protons. However,

Scheme 2[a]

[a] Reagents: HATU, HOAt, NMM, CH$_2$Cl$_2$/DMF.

Figure 4. NH stretch region FT-IR data for a 1.4 mM sample of the spiropseudodipeptide **6a** in CHCl$_3$.

it was tentatively assigned as trans on the basis of the fact that α-alkyl-substituted prolines are known to induce the trans form of the Xaa−Pro bond (Xaa = acyl, aminoacyl) preferentially because of unfavorable steric interactions between the alkyl groups and the α proton of Xaa in the cis form.[36,40] Thus, *N*-acetyl-2-methylproline-*N*′-methylamide has been shown to exist only in the trans conformation.[36]

As shown in Scheme 2, the HATU/HOAt promoted coupling of the side chain pseudodipeptides **9a**−**d** to the macrocyclic depsipeptides **10**[33] and **11**,[21] freshly prepared from their *N*-Boc-protected derivatives by treatment with a 4.6 M solution of HCl in EtOAc, led to the desired aplidine and tamandarin A analogues **4a**−**c** and **5a**−**d**, respectively. Unlike aplidine, the RP-HPLC and NMR analysis of these compounds did not show the presence of cis/trans isomers.

Conformational Analysis of the Spirolactam Aplidine Analogue 4a. Determination of the crystal structure of the aplidine analogue **4a** by X-ray diffraction analysis was not possible because suitable crystals could not be obtained. Unlike aplidine, the ^{1}H NMR spectra of compound **4a** in CDCl$_3$ or DMSO-d_6 solution showed the presence of only one preferred conformation. In Xaa-Pro-containing peptides the assignment of the cis or trans conformation at the peptide bond is based either on the NOE effects observed between the Xaa residue α-H and the Pro α-H in cis conformers, or δ-H in trans isomers,[38,41−44] or on the different anisotropic effects of the Xaa amide C=O group on the Pro carbons and protons at the α and δ positions in both isomers, which affect their respective chemical shifts.[36−38,41] None of these criteria could be applied to the assignment of cis/trans conformation at the (pyruvyl[9])−spirolactam amide bond in the aplidine analogue **4a**. The first is due to the absence of α-H in the pyruvyl[9] residue, and the second is because it requires the assignment of the chemical shifts of both isomers for their comparison. Therefore, as a tool for the assignment of the (pyruvyl[9])−spirolactam amide bond conformation, prior to the conformational analysis of **4a** by NMR and molecular modeling, we studied the conformational preference at that amide bond in the spirolactam side chain model, compound **6a**, as well as its preference for β- or γ-turn conformations.

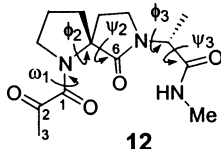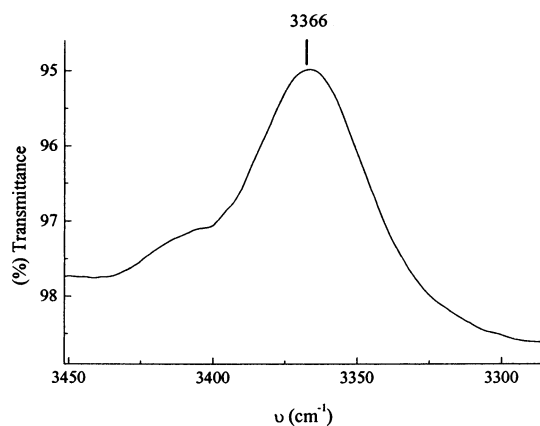**Conformational Analysis of the Spirolactam Pseudodipeptide 6a.** The NMR spectra of pseudo-

dipeptide **6a** showed the presence of two preferred conformations in variable ratios depending on the solvent (1:20 in CDCl$_3$, 1:8 in acetone-d_6, and 1:5 in DMSO-d_6). A trans conformation at the pyruvyl amide bond was assigned to the major conformer, based on the chemical shift comparison of both isomers.[36−38,41] Thus, as shown in Table 5, the 2-H protons (which correspond to the δ protons of Pro) of the minor conformer appeared shielded (3.52 and 3.56 ppm) with respect to those of the major isomer (3.68 and 3.82 ppm). Similarly, the C$_2$ signal of the minor conformer appeared shielded (49.01 ppm) with respect to that of the major one (50.21 ppm), while C$_5$ appeared more shielded in the major conformer (69.85 with respect to 70.21 ppm). To determine the possible existence of an intramolecular hydrogen bond between the methyl amide NH and one of the carbonyls, we studied the temperature dependence of that NH chemical shift between 35 and 55 °C in CDCl$_3$ and DMSO-d_6. In both solvents the Δδ/ΔT value of the major conformation was 4.4 ppb/K. This value did not conclusively establish the existence of a hydrogen bond and suggests that the NH is probably involved in an equilibrium between a hydrogen-bonded and a non-hydrogen-bonded state.[45,46] However, the low-field chemical shift of this NH in CDCl$_3$ (7.34 ppm), in addition to its small downfield shift (Δδ = 0.26 ppm) when CDCl$_3$ was replaced by DMSO-d_6, indicated a high degree of intramolecular hydrogen bonding.[45−47] Moreover, as shown in Figure 4 in the FT-IR spectra of **6a** at 1.4, 5, and 14 mM concentrations in CHCl$_3$, the NH stretching vibrations appeared as a strong broad band at 3366 cm^{-1} corresponding to a hydrogen-bonded amide proton and as a very weak shoulder above 3400 cm^{-1} corresponding to a small proportion of non-hydrogen-bonded amide protons. The shape and frequency of these NH stretching bands were concentration-independent, indicating the absence of aggregation and that the hydrogen bond was intramolecular.[46,48−51] Taking into account the preference for a trans conformation of the pyruvyl amide bond, two of the three carbonyls could participate as acceptors in the intramolecular hydrogen bond: either the pyruvic carboxamide group, forming a β-turn conformation, or the spirolactam carbonyl group, forming a γ-turn conformation.

The preference between the β- and γ-turn conformations was studied by molecular modeling calculations carried out on the spiropseudodipeptide analogue **12**

Table 1. Relevant Topographic Parameters of the Low-Energy Conformers for the Spiropseudodipeptide **12** and Ideal β and γ Turns

	ΔE	angle (deg)					distances (Å)			
conformer	(kcal/mol)	ω_1	ϕ_2	ψ_2	ϕ_3	ψ_3	C_1O-HN	C_6O-HN	C_2-Me^a	$(3\text{-H})-Me^b$
12a	0	177.15	−52.3	133.7	101.4	−37.6	2.18	3.20	5.92	3.97
12b	3.2	177.72	−62.0	121.9	−82.1	61.5	5.46	2.14	8.90	9.31
β II turn[c]			−60	120	80	0			<7	
γ turn[d]					−76	76				

[a] Distance between pyruvyl C_2 and the methyl amide carbon. [b] Distance between pyruvyl 3-H and Me protons. [c] Ideal β II turn. [d] Ideal inverse γ turn.

(Table 1), where the D-Leu residue was replaced by D-Ala to simplify the calculations. The conformational space of this pseudodipeptide was explored by simulated annealing molecular dynamics, followed by minimization, employing the AMBER force field[52,53] and using the model-building facility implemented in Insight II to construct the initial molecular models. The obtained minima were compared, and the repeated ones were eliminated. Unique minima were clustered into families according to their heavy atom rms values and peptide backbone torsion angle values and were analyzed for the presence of β and γ turns. Additionally, because the previous NMR study had shown the presence of cis and trans rotamers for the pyruvyl−spirolactam amide bond, the corresponding dihedral angle (ω_1) was also analyzed. Among the resulting structures, only 6% had a cis conformation at that amide bond, and all of these were at least 2 kcal mol^{-1} above the global minimum. The low-energy conformers found within a 2 kcal mol^{-1} energy window from the global minima (88%), all of them corresponding to trans isomers, were clustered into six families. Optimization using the semiempirical AM1 Hamiltonian,[54] as implemented in the MOPAC module of the Insight II program package, was carried out. This led to two families of conformers whose most significant topographic parameters are shown in Table 1. The calculated dihedral angles and distances for conformers **12a** (69% of the frames) are in good correlation with those expected for a β II turn conformation.[55−57] Thus, the distance between the pyruvyl C_2 (which corresponds to the $C_{\alpha i}$ of the β turn) and the methyl amide carbon (which corresponds to the $C_{\alpha i+3}$ of the β turn) was less than 7 Å (5.92 Å), in accordance with one of the most significant criteria for the definition of β turns.[46,56] In addition, the value of 2.18 Å for the distance between the pyruvyl amide oxygen and the methyl amide HN, less than than 2.5 Å, supports the existence of a hydrogen bond in conformers **12a**.[46] With respect to the dihedral angles, the difference between the calculated value for ψ_3 for these conformers and that of an ideal β II turn (−37.64°) was higher than the generally accepted window of ±30°; however, differences of up to ±45° for this torsion angle have been also reported.[56,58] On the other hand, the calculated values for the ϕ_3 and ψ_3 dihedral angles for **12b** conformers (31% of the frames), as well as the distance between the spirolactam carbonyl oxygen and the methyl amide HN (2.14 Å), correspond to those of a hydrogen-bonded inverse γ turn centered at the D-Ala residue ($i + 1$

residue of the γ turn). The presence of a weak NOE effect between pyruvyl 3-H and the methyl protons of the methyl amide, observed in the CDCl$_3$ 1D NOESY spectrum of the pseudodipeptide **6a**, is compatible only with a β turn conformation, since the distance calculated for those protons in conformer **12b** (9.31 Å) is too long for that NOE to be observed. Therefore, the combined results of the NMR, FT-IR, and molecular modeling studies support the high preference for a β II turn conformation in the spiropseudodipeptide **6a**.

NMR Analysis of the Spirolactam Aplidine Analogue 4a. As already mentioned, the NMR spectra of the aplidine analogue **4a** in CDCl$_3$ and DMSO-d_6 solution showed the presence of only one preferred conformation whose proton and carbon resonances were completely assigned on the basis of 2D COSY, TOCSY, NOESY, HSQC, and HMBC experiments. This assignment was confirmed with 2D HSQC-TOCSY spectra (^{1}H and ^{13}C chemical shifts are included in Table 1 of the Supporting Information). Although the pyruvyl−spirolactam amide bond conformation could not be directly established from these NMR data, it was assigned as trans based on the high preference for a trans conformation at this amide bond, determined in the model spiropseudodipeptide **6a**. Moreover, the ^{1}H and ^{13}C NMR data of the spirolactam unit of **4a** were more similar to those of the trans isomer of **6a** than to those of the cis isomer.
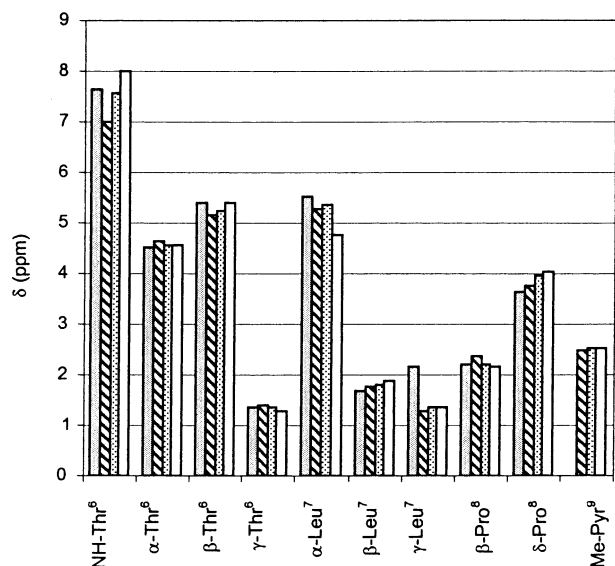
A comparison of ^{1}H and ^{13}C chemical shifts of the restricted aplidine analogue **4a** in CDCl$_3$ with those described for didemnin B[26] (**1**) and both cis and trans conformations of aplidine[27] (**2**) did not indicate significant differences at the macrocycle residues. Concerning the side chain residues, the most significant differences were found at the (Thr^6) NH and β-H and at the (Leu^7) α-H protons (Figure 5). In the first case, the differences at the (Thr^6) protons could be related to the higher strength of the hydrogen bond between the (pyruvyl^9) carboxamide carbonyl group and the (Thr^6) NH in **4a** than in aplidine or didemnin B (see below), while in the case of the (Leu^7) α-H the differences could be attributed to the local modification that the spirolactam introduces into this residue. In the overall comparison of chemical shifts, the data of the restricted compound **4a** were more similar to those of *trans*-aplidine than to those of the cis isomer.

As shown in Table 2, the temperature coefficients determined in the study of temperature dependence of amide proton chemical shifts for the restricted aplidine

Table 2. Temperature Dependence of the NH Chemical Shifts of Didemnin B, *cis*- and *trans*-Aplidine and **4a**, Given as $-\Delta\delta/\Delta T$ (ppb/K)
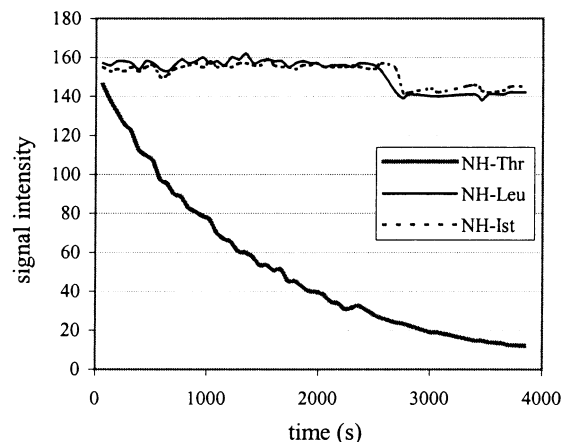
| | didemnin B[a] | | *cis*-aplidine[c] | *trans*-aplidine[c] | **4a** | |
NH	$CDCl_3$[a]	DMSO-d_6[b]	$CDCl_3$	$CDCl_3$	$CDCl_3$[d]	DMSO-d_6[e]
(Ist[1])	1.70	0.5	2.00	2.00	0.44	0.70
(Leu[3])	2.20	1.8	2.20	2.20	0.37	1.22
(Thr[6])	4.25	4.3	3.51	4.80	0.89	3.36

[a] Reference 26. [b] Reference 25. [c] Reference 27. [d] Determined by measuring the chemical shifts between 25 and 57.5 °C with intervals of 6.5 °C. [e] Determined by measuring the chemical shifts between 25 and 75 °C with intervals of 10 °C.

Figure 5. Comparison of ^{1}H NMR chemical shifts of the side chain residues: (shaded bar) didemnin B; (cross-hatched bar) *cis*-aplidine; (dotted bar) *trans*-aplidine; (clear bar) aplidine spirolactam analogue **4a**.

Figure 6. Proton−deuterium exchange kinetics for compound **4a** in MeOH-d_4.

Table 3. Observed Interresidue NOE Correlations for the Aplidine Analogue **4a**[a]

(Ist[1])	(Hip[2])	(Leu[3])	(Pro[4])	(Me₂Tyr[5])	(Thr[6])	(Leu[7])	(Spirolactam)	(Pyruvyl[9])
NH			α-H	N-CH₃	NH			
NH					α-H			
NH				α-H				
NH				N-CH₃				
NH							8-H	
4-H							8-H	
2-H		NH	α-H	N-CH₃				
7-H		NH	β-H	aromatics				
	2-H	NH		aromatics			8-H	
	2-CH₃	NH		aromatics			2-H	
				NH	α-H			
		α-H	δ-H	N-CH₃	α-H			
		α-H			NH			
		α-H			γ-H			
		α-H				β-H		
					NH	α-H		
						NH	8-H	
						β-H		CH₃

[a] Observed in the NOESY spectra registered in CDCl₃ at 500 MHz (mixing times: 500 and 750 ms).

analogue **4a** in CDCl₃ were significantly lower than those described for didemnin B[26] and both cis and trans conformations of aplidine.[27] The three low values obtained for the temperature coefficients of **4a** are characteristic of strongly hydrogen-bonded amide protons.[45,46] In particular, it is noteworthy that the value obtained for the (Thr[6]) NH (0.89 ppb/K) is much lower than the corresponding values described for didemnin B (4.25 ppb/K)[26] and *cis*- and *trans*-aplidine (3.51 and 4.8 ppb/K).[27] As expected, the temperature coefficients in DMSO-d_6 were higher than in CDCl₃ but within the normal values for hydrogen-bonded NHs.[45,51] Furthermore, the low solvent dependence of the NH chemical shifts from CDCl₃ to DMSO-d_6 [0.24 ppm for (Ist[1]), 0.08 ppm for (Leu[3]), and 0.06 ppm for (Thr[6])] indicated the low accessibility of the solvent to these NHs.[52] This low accessibility was also deduced from the study of proton−deuterium exchange in MeOH-d_4. As shown in Figure 6, the (Ist[1]) and (Leu[3]) NHs did not exchange with deuterium after being dissolved in MeOH-d_4 for 1 h, which indicated an internal orientation of these NHs, making them completely inaccessible to the solvent, while the slow exchange of (Thr[6]) NH suggests its participation in a hydrogen bond but in slow equilibrium with a nonbonded state.

As in the case of didemnin B[25,26] and aplidine,[27] the sequential NOE correlations observed in the NOESY spectra between the NH or NCH₃ and the α proton of the preceding residue and between (Leu[3]) α-H and (Pro[4]) δ-H allowed the assignment of a trans conformation to all peptide bonds in **4a** (Table 3). Moreover, the most significant nonsequential NOEs observed between the macrocycle residues were also in good agreement with those reported for both cis and trans conformations of aplidine and for didemnin B in CDCl₃, indicating that the three-dimensional structure of the macrocycle is similar in all cases. Thus, the cross-peaks of (Ist[1]) NH with (Pro[4]) α-H, (Me₂Tyr[5]) α-H, and N-Me protons supported the participation of that NH in a hydrogen bond, forcing the macrocycle into the figure of eight shape, and the cross-peaks of (Leu[3]) NH with (Thr[6]) α-H and (D-Leu[7]) α-H, as well as (Leu[3]) α-H with (Thr[6]) NH and (D-Leu[7]) β-H, supported the presence of the (Leu[3]) NH → (D-Leu[7]) C=O hydrogen bond and the folding back of the side chain toward the macrocycle. This folding was also indicated by the NOE correlations of the spirolactam 8-H protons (corresponding to the N-Me of aplidine Leu[7]) with the (Ist[1]) NH and 4-H protons.

With respect to the side chain, the NOE pattern was also similar to that of aplidine and in good agreement with that expected for a β II turn conformation. Thus, strong NOE correlations were observed between (Leu[7]) α-H and (Thr[6]) NH, the spirolactam 8-H and (Thr[6]) NH, and the spirolactam 4-H protons (which correspond to Pro[8] β-H of aplidine), and between the pyruvyl 3-H protons and (Thr[6]) β-H and γ-H. The overall NOE correlation pattern did not change from CDCl$_3$ to DMSO-d_6, indicating the absence of significant conformational variability with the solvent.

Molecular Mechanics/Dynamics Calculations for Spirolactam Aplidine Analogue 4a. Owing to the inherent lack of precision associated with the determination of interproton distances in molecules of the size of aplidine by NMR techniques,[59] in addition to the limited number of interatomic distances per residue accessible experimentally, molecular mechanics/dynamics calculations were carried out in order to provide more information on the three-dimensional structure of the spirolactam aplidine analogue **4a** and to examine its conformational preferences. Calculations were performed using the well-established CHARMm force field[60,61] at 300K for reasonably long periods of time (see Experimental Section) and without distance restraints in order to allow the molecule to more fully explore the conformational space available to it. Three implicit solvent descriptions ($\epsilon = 4.8$, 45, and 80) and two explicit solvent models (H$_2$O and DMSO) were applied. Tables of derived quantities (interatomic distances, torsion angles, and hydrogen-bonding patterns) resulting from these calculations are included in the Supporting Information (see Tables 2–4 in the Supporting Information).

Good agreement was observed between the interatomic distances derived from the unrestrained molecular dynamics trajectories in the CHARMm all-atom representation and the NOE-derived distances from the experimental NMR data. Nearly all of the atomic distances that corresponded to the measured NOE distances were within those values that would be expected to produce an NOE (see Table 2 in the Supporting Information).

Analysis of the most relevant torsion angles found in the simulations indicates that the overall three-dimensional structure of the spirolactam aplidine analogue **4a** is similar to that of the trans isomer of aplidine.[27] Furthermore, comparison with reported results for didemnin B by NMR studies[25] and by X-ray diffraction[24] indicates that the three-dimensional structures of all three molecules are similar, the macrocycle in each case adopting a twisted figure eight conformation.

The hydrogen-bonding patterns detected in the simulations show that the transannular hydrogen bond between (Ist[1]) NH and (Leu[3]) CO is present in almost all simulations, as is that between (Leu[3]) NH and (MeLeu[7]) CO. This result is compatible with the low $\Delta\delta/\Delta T$ values observed by ^{1}H NMR for the (Ist[1]) NH and (Leu[3]) NH protons, respectively (see Table 2). These hydrogen bonds, also present in aplidine and in didennin B, are responsible for the above-mentioned figure eight disposition of the macrocycle. In the present study another transannular hydrogen bond between (Leu[3]) NH and (Ist[1]) CO is also detected in all simulations. In
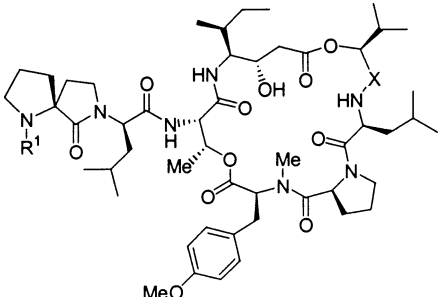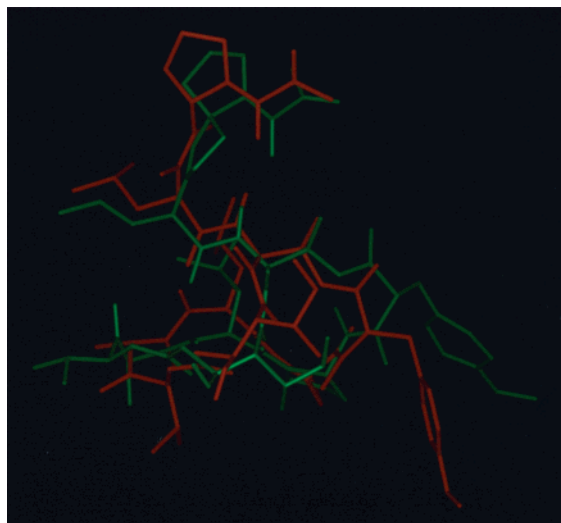

Figure 7. Superposition of the representative snapshots from the trajectories of the DMSO explicit-solvent simulations for the aplidine spirolactam analogue **4a** (green) and *trans*-aplidine (orange).

the molecule's side chain, a hydrogen bond between (Thr[6]) NH and (pyruvyl[9]) carboxamide CO, analogous to that found in aplidine[27] and to that found in didemnin B between (Thr[6]) NH and (Lac[9]) CO,[24] is found in all simulations. Another hydrogen bond between (Thr[6]) NH and (spirolactam) CO is also detected. These hydrogen bonds stabilize β- and γ-type turns, respectively, in the molecule's side chain. This result is also compatible with the low $\Delta\delta/\Delta T$ value observed for the (Thr[6]) NH proton, as shown in Table 2.

The similarity of the three-dimensional structure of the spirolactam analogue of aplidine **4a** to that of aplidine and to that of didemnin B is illustrated by the superposition of representative snapshots from the trajectories of the DMSO explicit-solvent simulations of both these molecules and with the reported X-ray crystal structure of didemnin B as shown in Figures 7 and 8. Only those atoms belonging to the macrocycle in each case were aligned, minimizing the root-mean-square differences. The rmsd values of 1.1228 and 0.7319 Å, respectively, were obtained between the spirolactam analogue **4a** and aplidine on one hand and between **4a** and didemnin B on the other.

Biological Results and Discussion. The cytotoxicity of the conformationally restricted spirolactam didemnin analogues **4** and **5** in human lung carcinoma (A549) and human colon carcinoma (HT-29) cell lines was determined as previously described.[62] For comparative purposes, didemnin B (**1**), aplidine (**2**), tamandarin A (**3**), and dehydrotamandarin A were also included in the assay. As indicated in Table 4, all the new compounds were less cytotoxic than the model compounds and, similarly to other didemnin congeners, none of them showed selectivity for either of the two cell lines assayed.[18] The conformation restriction introduced to enforce the β-turn conformation in the linear side chain of aplidine led to a 20- and 50-fold decrease in the cytotoxicity of the spirolactam contianing **4a** against HT-29 and A549 cells, respectively. An even more marked decrease (200-fold) was found in the cytotoxicity of **5a** with respect to that of dehydrotamandarin A.

Table 4. Cytotoxicity of Conformationally Restricted Didemnin Analogues **4** and **5**

compd	R[1]	X	IC$_{50}$ (nM) A549[a]	HT-29[b]
didemnin B (**1**)[c]	(*S*)-Lac	(*S*)-[COCH(CH$_3$)CO]	2	2
aplidine (**2**)	pyruvyl	(*S*)-[COCH(CH$_3$)CO]	0.18	0.45
tamandarin A (**3**)	(*S*)-Lac	CO	0.95	0.95
dehydrotamandarin A	pyruvyl	CO	0.47	0.47
4a	pyruvyl	(*S*)-[COCH(CH$_3$)CO]	8.55	8.90
4b	isobutyryl	(*S*)-[COCH(CH$_3$)CO]	89.1	89.1
4c	Boc	(*S*)-[COCH(CH$_3$)CO]	8.68	8.68
5a	pyruvyl	CO	93.8	93.8
5b	isobutyryl	CO	93.8	93.8
5c	Boc	CO	4.56	4.56
5d	2-Me-acryloyl	CO	93.9	93.9

[a] A549 = human lung carcinoma cells. [b] HT-29 = human colon carcinoma cells. [c] Values reported in ref 18.
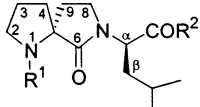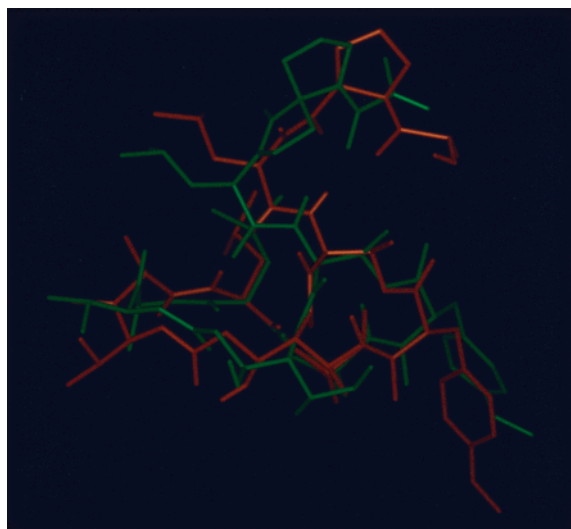

Figure 8. Superposition of the representative snapshots from the trajectories of the DMSO explicit-solvent simulations for the aplidine spirolactam analogue **4a** (green) and the X-ray crystal structure of didemnin B (orange).

Taking into account the results of the conformational analysis of the aplidine analogue **4a** in comparison with aplidine, the decrease in the cytotoxicity produced by the spirolactam conformational constraint cannot be related either to changes in the macrocycle conformation or to an inefficient induction of the preferred β II turn conformation in the side chain. As mentioned above, apart from the lower flexibility of the side chain in the restricted analogue **4a**, the most significant difference is that, unlike aplidine in which the cis and trans rotamers around the pyruvyl[9]−Pro[8] amide bond are similarly stabilized,[27,28] the (pyruvyl[9])−spirolactam amide bond essentially adopts the trans form in **4a**. This fact strongly suggests the preference for the pyruvyl[9]−Pro amide cis isomer in the bioactive conformation of aplidine. In view of the overall 3D structural similarity between didemnin B and compound **4a**, including the

high preference for the trans rotamer at the Xaa[9]−Pro[8] amide bond, the lower flexibility at the side chain in **4a** could account for its 4-fold lower cytotoxicity.

Although a thorough conformational analysis of compounds **4b**, **4c**, and **5a**−**d** has not been carried out, the importance of the R[1]−Pro[9] bond in a cis conformation would explain the considerable differences in cytotoxicity between the *N*-acyl derivative **4b** or **5b** and their corresponding *N*-urethanyl analogue **4c** or **5c** in both series. Since no evidence of a mixture of rotamers was detected either in the model isobutyryl **8b** and **9b** or in the final macrocycle derivative **4b** and **5b**, it is reasonable to assume that these latter compounds, which are among the least cytotoxic spirolactam derivatives, do exist in a trans conformation, as discussed above. In contrast, on the basis of the preference for the cis rotamer in the model Boc derivative **9c** and the literature data,[39] we presume that the only rotamer detected in the macrocyclic analogues **4c** and **5c**, among the most cytotoxic spirolactam derivatives, is also in this conformation. It is interesting to note that compound **5c**, which showed the highest cytotoxicity among all these spirolactams, is less cytotoxic than tamandarin A and dehydrotamandarin A by only 5- and 10-fold, respectively. Finally, the decrease in cytotoxicity of the spirolactam containing the 2-Me-acryloyl moiety **5d** could also be attributed to the adoption of the (2-Me-acryloyl)[9]−Pro[8] amide bond only in the trans conformation, as demonstrated in the model compounds **8d** and **9d**.

The significant influence of the Xaa[9]−Pro[8] amide bond cis/trans isomerism upon the cytotoxic activity of didemnins, herein commented, suggests the possible participation of a peptidyl−prolyl cis/trans isomerase in their mechanism of action. This participation has been previously suggested to explain the immunosuppressive effects of didemnin B,[3,63] although, unlike the macrocyclic immunosuppressants cyclosporin A (CsA), FK506, and rapamycin, a didemnin B specific immunophilin has not been identified. The first step in the

Table 5. Relevant Analytical and Spectroscopic Data of Spirolactam Pseudodipeptides

	6a	8a	8b	8d	9a	9b	9c	9d
R^1	pyruvyl	pyruvyl	isobutyryl	2-Me-acryloyl	pyruvyl	Isobutyryl	Boc	2-Me-acryloyl
R^2	NHCH$_3$	OBn	OBn	OBn	H	H	H	H
yield (%)	76	56	74	50	95	95	64	85
mp (°C)	syrup	syrup	87	syrup	amorphous	68−69	192−194	amorphous
formula[a]	$C_{17}H_{27}N_3O_4$	$C_{23}H_{30}N_2O_5$	$C_{24}H_{34}N_2O_4$	$C_{24}H_{32}N_2O_4$	$C_{16}H_{24}N_2O_5$	$C_{17}H_{28}N_2O_4$	$C_{18}H_{30}N_2O_5$	$C_{17}H_{26}N_2O_4$
t_R (min) (A/B)[b]	3.60 (30/70)	5.87, 6.72 (50:50)	4.50 (50:50)	6.38 (50:50)	13.14 (20:80)	ND[c]	13.41 (50:50)	6.38 (25:75)
[α]$^{20}_D$	+69.4 (c 1, MeOH)	ND[c]	+9.6 (c 1, MeOH)	ND[c]	+3.5 (c 1, MeOH)	−2 (c 1.1, MeOH)	−3 (c 1, MeOH)	+18.8 (c 1, MeOH)
ESI-MS (m/e)	338.3 [M + H]$^+$	415.4 [M + H]$^+$	415.4 [M + H]$^+$	413.3 [M + H]$^+$	325.1 [M + H]$^+$	323.3 [M−H]$^+$	353.4 [M − H]$^+$	323.2 [M + H]$^+$

^{1}H NMR[d]	6a major[e] (trans)	6a minor[f] (cis)	8a major[e] (trans)	8a minor[f] (cis)	8b	8d	9a major[e] (trans)	9a minor[f] (cis)	9b	9c	9d
2-H	3.68, 3.82	3.52, 3.56	3.56−3.78	3.92	3.60−3.70	3.56−3.68	3.58−3.70	3.86	3.61−3.75	3.30	3.57−3.67
3-H	1.86−2.20		1.61−2.39		1.61−2.10	1.64−1.93	1.64−1.82		1.90−2.10	1.70−1.90	1.55−2.25
4-H	1.86−2.20		1.61−2.39		1.61−2.10	1.96−2.12	1.86−2.18		1.90−2.10	1.70−1.90	3.57−3.67
8-H	3.37		3.22, 3.56−3.78		3.14, 3.60−3.70	3.20, 3.56−3.68	3.46	3.35	3.30, 3.49	3.10, 3.70	3.19−3.44
9-H	1.86−2.20, 2.51		1.61−2.39, 2.77		1.61−2.10, 2.64	1.64−1.93, 2.78	1.86−2.18, 2.60−2.74		1.90−2.10, 2.49	1.70−1.90, 2.50	1.55−2.25, 2.56
α-H	4.85	4.50	4.85	4.67	4.85	4.80	4.80	4.73	4.71	4.39	4.78
β-H	1.62, 1.91		1.61−2.39		1.61−2.10	1.64−1.93	1.71−2.22		1.70	1.64	1.55−2.25
R^1	2.38	2.29	2.44	2.27	1.09, 1.12[g]	5.19[h]	2.39	2.30	1.09, 1,12[g]	1.36	5.18[h]

^{13}C NMR[i]	6a major[e] (trans)	6a minor[f] (cis)	8a major[e] (trans)	8a minor[f] (cis)	8b	8d	9a major[e] (trans)	9a minor[f] (cis)	9b	9c	9d
C$_2$	50.21	49.01	48.91	47.72	47.87	50.19	49.30	48.03	48.04	48.19	50.51
C$_3$	25.73	25.79	24.92	24.76	24.86	24.22	24.93	24.70	25.01	22.59	24.61
C$_4$	37.45	37.37	36.47	35.63	35.76	37.09	36.01	36.60	36.55	36.87	37.43
C$_5$	69.85	70.21	66.83	67.03	67.55	66.81	69.11		67.57	67.29	67.49
C$_8$	40.83	41.14	40.77		40.49	41.11	41.01	41.31	40.64	40.59	40.94
C$_9$	29.49		29.31	32.31	29.55	29.97	29.90	32.50	30.78	30.45	30.13
C$_α$	54.54		52.90	53.18	52.71	53.24	53.42	53.58	53.46	54.32	53.72
C$_β$	36.81		37.28	37.39	37.62	37.70	37.01	37.44	36.94	38.18	37.82
R^1	27.17	27.58	26.94	26.94	18.64[g]	115.91[h]	27.09	26.79	18.65[g]	28.54	116.27[h]
	201.45	198.70	198.04	197.65			197.49	197.49			

^{a} Satisfactory analyses for C, H, N. ^{b} NovapacK C$_{18}$ (3.9 mm × 150 mm, 4 μm), A = CH$_3$CN, B = 0.05% TFA in H$_2$O. ^{c} Not determined. ^{d} Spectra registered at 300 MHz in CDCl$_3$ except for **6a** (acetone-d_6) and **9c** (DMSO-d_6, 90 °C). Spectra assignment based on COSY and HSQC spectra. ^{e} Major rotamer at the pyruvyl amide bond. ^{f} Minor rotamer at the pyruvyl amide bond. ^{g} δ for the R^1 = CH$_3$. ^{h} δ for the R^1 = CH$_2$. ^{i} Spectra registered at 75 MHz in CDCl$_3$ except for **6a** (acetone-d_6).

intracellular action of cyclosporin A, FK-506, and rapamycin is their binding to their specific peptidyl−prolyl isomerases, cyclophilin A (CsA), and FK506-binding proteins (FK506 and rapamycin).[3,64,65] Besides their fundamental role in protein folding,[66] peptidyl−prolyl isomerases are crucial in signal transduction, cell cycle regulation, and receptor trafficking and assembly[65−68] so that interference of didemnins with peptidyl−prolyl isomerase activity might be related to their antitumoral and immunosuppressive effects.

Experimental Section

General Synthetic Methods. All reagents were of commercial quality. Solvents were dried and purified by standard methods. Amino acid derivatives were obtained from Bachem Feinchemikalien AG. Analytical TLC was performed on aluminum sheets coated with a 0.2 mm layer of silica gel 60 F$_{254}$, Merck, and preparative TLC was performed on 20 cm × 20 cm glass plates coated with a 2 mm layer of silica gel PF$_{254}$, Merck. Silica gel 60 (230−400 mesh), Merck, was used for flash chromatography. Preparative radial chromatography was performed on 20 cm diameter glass plates coated with a 2 mm layer of silica gel PF$_{254}$, Merck. Melting points were taken on a micro-hot-stage apparatus and are uncorrected. ^{1}H NMR spectra were recorded with Varian Gemini-200, Varian INOVA-300, or Varian INOVA 400 spectrometer, operating at 200, 300, or 400 MHz, using TMS as reference. ^{13}C NMR spectra were recorded with Varian Gemini-200 or Varian INOVA 400

spectrometers, operating at 50 or 100 MHz. Elemental analyses were obtained on a CH-O-RAPID apparatus. Analytical RP HPLC was performed on Waters μBondapak C$_{18}$ (3.9 mm × 300 mm, 4 μm) or Novapak C$_{18}$ (3.9 mm × 150 mm, 4 μm) columns with a flow rate of 1 mL/min and using a tunable UV detector set at 214 nm. Mixtures of CH$_3$CN (solvent A) and 0.05% TFA in H$_2$O (solvent B) were used as mobile phases. Analytical and preparative HPLC of the final peptides was performed on a ThermoQuest HyperPrep PEP 100 C$_{18}$ (250 mm × 21 mm) column with a flow rate of 7 mL/min, using a tunable UV detector set at 270 nm. Mixtures of CH$_3$CN and 0.05% TFA in H$_2$O were used as mobile phases in isocratic mode. Optical rotations were measured on a Perkin-Elmer 141 polarimeter. ESI-MS experiments were performed, in positive mode, on a Hewlett-Packard 1100 MSD apparatus.

Synthesis of (5R)-7-[(1R)-1-Benzyloxycarbonyl-3-methylbutyl]-6-oxo-1-pyruvyl-1,7-diazaspiro[4.4]nonane (8a). Method A. Pyruvic acid (19.2 mg, 0.22 mmol), HATU (100 mg, 0.26 mmol), HOAt (35 mg, 0.26 mmol), and NMM (48 μL, 0.44 mmol) were successively added, under argon, to a 0 °C cooled solution of freshly prepared trifluoroacetate **7**^{32} (101 mg, 0.22 mmol) in dry CH$_2$Cl$_2$ (5 mL). After 24 h of stirring at room temperature, the reaction mixture was diluted with CH$_2$Cl$_2$ (5 mL), and the solution was successively washed with 10% citric acid solution (5 mL), saturated NaHCO$_3$ (5 mL), and brine (5 mL), dried over Na$_2$SO$_4$, and evaporated to dryness. The residue was purified by radial chromatography, using (1:3) hexane/EtOAc as eluant to give the title pseudodipeptide derivative **8a** as a syrup (42 mg, 47%), whose significant analytical and spectroscopic data are shown in Table 5.

Method B. Triethylamine (280 μL, 1.98 mmol) and DMAP (4 mg, 33 μmol) were added to a 0 °C cooled solution of freshly prepared trifluoroacetate **7**[32] (151 mg, 0.33 mmol) in dry CH$_2$Cl$_2$ (4 mL). This mixture was slowly added to a solution of pyruvyl chloride, freshly prepared from pyruvic acid (115 mg, 1.31 mmol) and dichloromethyl methyl ether (188 mg, 1.57 mmol) as previously described,[34] in CH$_2$Cl$_2$ (3 mL). The resulting reaction mixture was stirred at room temperature for 6 h and diluted with CH$_2$Cl$_2$ (10 mL). The solution was successively washed with 10% citric acid solution (5 mL), saturated NaHCO$_3$ (5 mL), and brine (5 mL), dried over Na$_2$SO$_4$, and evaporated to dryness. The residue was purified as in method A to yield the derivative **8a** (77 mg, 56%).

General Procedure for the Synthesis of *N*-Acyl Spirolactam Pseudodipeptides 8b and 8d. Triethylamine (283 μL, 2 mmol), DMAP (6.1 mg, 50 μmol), and the corresponding acyl chloride [isobutyryl chloride (106 mg, 1 mmol) or 2-methylacryloyl chloride (103 mg, 1 mmol)] were successively added to a 0 °C cooled solution of freshly prepared trifluoroacetate **7**[32] (228 mg, 0.50 mmol) in dry CH$_2$Cl$_2$ (10 mL). After 24 h of stirring at room temperature, the reaction mixture was diluted with CH$_2$Cl$_2$ (10 mL). The solution was successively washed with 10% citric acid solution (5 mL), saturated NaHCO$_3$ (5 mL), and brine (5 mL), dried over Na$_2$SO$_4$, and evaporated to dryness. The residue was purified by flash chromatography, using a 20−100% gradient of EtOAc in hexane as eluants. The most significant analytical and spectroscopic data of the title compounds **8b** and **8d** are summarized in Table 5.

General Procedure for the Hydrogenolysis of the Benzyl Esters 8a and 8b. Synthesis of the C-Deprotected Pseudodipeptides 9a and 9b. A sample of 10% Pd/C (30 mg) was added to a solution of the corresponding benzyl ester **8a** and **8b** (0.3 mmol) in MeOH (30 mL), and the mixture was hydrogenated at room temperature and 1 atm of H$_2$ pressure for 1 h. The catalyst was filtered off and washed with MeOH (5 mL), and the solution was evaporated to dryness. The residue was dissolved in H$_2$O (3 mL), and the resulting solution was lyophilized to give the C-deprotected pseudodipeptides **9a** and **19b** as white solids, whose analytical and spectroscopic data are summarized in Table 5.

Synthesis of (5*R*)-7-[(1*R*)-1-(*N*-Methyl)carbamoyl-3-methylbutyl]-6-oxo-1-pyruvyl-1,7-diazaspiro[4.4]nonane (6a). Pseudodipeptide **9a** (32 mg, 0.10 mmol), BOP (53 mg, 0.12 mmol), and NMM (22 μL, 0.20 mmol) were successively added, under argon, to a −5 °C cooled solution of methylamine hydrochloride (6 mg, 0.09 mmol) in dry CH$_2$Cl$_2$ (2 mL). After 2 h of stirring at −5 °C and 20 h at room temperature, the reaction mixture was diluted with CH$_2$Cl$_2$ (2 mL), and the solution was successively washed with 10% citric acid solution (2 mL), saturated NaHCO$_3$ (2 mL), and brine (2 mL), dried over Na$_2$SO$_4$, and evaporated to dryness. The residue was purified by radial chromatography, using a 30−50% EtOAc gradient in hexane as eluant, to give the title pseudodipeptide derivative **6a** as a syrup (25 mg, 76%), whose significant analytical and spectroscopic data are shown in Table 5.

Synthesis of (5*R*)-1-(*tert*-Butoxycarbonyl)-7-[(1*R*)-1-carboxy-3-methylbutyl]-6-oxo-1,7-diazaspiro[4.4]nonane (9c). Tetramethylammonium hydroxide pentahydrate (158 mg, 0.87 mmol) and di(*tert*-butyl) dicarbonate (144 mg, 0.66 mmol) were added to a solution of freshly prepared trifluoroacetate **7**[32] (150 mg, 0.44 mmol) in acetonitrile (5 mL). After 48 h of stirring at room temperature, the solvent was evaporated to dryness, and the residue was dissolved in CH$_2$Cl$_2$ (3 mL). The solution was extracted with H$_2$O (5 mL), and the extracts were lyophilized. The resulting residue was purified by flash chromatography, using an 8−40% gradient of MeOH in CH$_2$Cl$_2$ as eluant, to give the title compound **9c** as a white solid (100 mg, 64%), whose analytical and spectroscopic data are summarized in Table 5.

Synthesis of (5*R*)-7-[(1*R*)-1-Carboxy-3-methylbutyl]-1-(2-methylacryloyl)-6-oxo-1,7-diazaspiro[4.4]nonane (9d). A sample of 0.1 N NaOH (2.2 mL, 0.22 mmol) was added to a solution of the benzyl ester **8d** (83 mg, 0.2 mmol) in MeOH (3 mL), and the mixture was stirred at room temperature for 1

h. Afterward, the MeOH was evaporated, and the residue was dissolved in H$_2$O (10 mL). This aqueous solution was successively washed with CH$_2$Cl$_2$ (10 mL), acidified with 0.1 N HCl to pH 2, and extracted with CH$_2$Cl$_2$ (3 × 20 mL). The combined organic extracts were washed with brine (20 mL), dried over Na$_2$SO$_4$, and evaporated to dryness to yield the title pseudodipeptide **9d** as a white amorphous solid (55 mg, 85%), whose significant analytical and spectroscopic data are summarized in Table 5.

General Procedure for the Synthesis of Spirolactam Pseudodepsipeptides 4a−c and 5a−d. The corresponding pseudodipeptides **9a-d** (14 μmol), HATU (12.4 mg, 32 μmol), HOAt (4.5 mg, 33 μmol), and NMM (3.3 μL, 30 μmol) were successively added, under argon, to a −5 °C cooled solution of the respective macrocyclic depsipeptide hydrochlorides **10**[33] and **11**[21] (freshly prepared from 13 μmol of their *N*-Boc-protected derivatives by treatment with 50 μL of 4.6 M HCl solution in EtOAc) in a (2:1) CH$_2$Cl$_2$/DMF mixture (150 μmol). The resulting mixture was stirred, first for 2 h at −5 °C and then for 14 h at room temperature. Afterward, the solvent was evaporated, and the residue was treated with EtOAc (2 mL). The precipitate was filtered off, and the solution was washed successively with 10% KHSO$_4$ (2 × 1 mL), H$_2$O (1 mL), a saturated solution of NaHCO$_3$ (1 mL), and brine (1 mL), dried over Na$_2$SO$_4$, and evaporated to dryness. The residue was purified by preparative HPLC performed on a HyperPrep PEP 100 C$_{18}$ (250 mm × 21 mm) column with a flow rate of 7 mL/min, using a (85:15) CH$_3$CN/0.05% TFA mixture as eluant.

[(5*R*)-7-[(1*R*)-1-Carbonyl-3-methylbutyl]-6-oxo-1-pyruvyl-1,7-diazaespiro[4.4]nonane$^{7-9}$]aplidine (4a). White amorphous solid (9 mg, 63%). HPLC [HyperPrep PEP 100 C$_{18}$ (A/B, 85:15), ϕ = 7 mL/min] t_R = 14.4 min. ^{1}H NMR (300 MHz, CDCl$_3$): δ 0.90−1.00 (m, 24 H), 1.05−1.40 (m, 12 H), 1.40−2.25 (m, 16H), 2.27−2.41 (m, 1H), 2.42−2.70 (m, 3H), 2.54 (s, 3H), 2.92−2.98 (m, 1H), 3.12−3.38 (m, 4 H), 3.54−3.78 (m, 4 H), 3.79 (s, 3H), 4.01−4.12 (m, 2H), 4.20−4.26 (m, 2H), 4.57−4.62 (m, 2H), 4.77−4.82 (m, 2H), 5.18 (d, 2H, J = 3 Hz), 5.37−5.42 (m, 1H), 6.84 (d, 2H, J = 9 Hz), 7.07 (d, 2H, J = 9 Hz), 7.20 (d, 1H, J = 10 Hz), 7.85 (d, 1H, J = 10 Hz), 7. 87 (d, 1H, J = 5 Hz). ^{13}C NMR (75 MHz, CDCl$_3$): δ 11.86, 14.97, 15.47, 16.78, 17.12, 18.84, 21.20, 21.27, 23.62, 24.14, 15.03, 25.15, 25.30, 27.35, 27.51, 28.19, 30.46, 31.52, 34.27, 35.95, 39.01, 40.07, 41.59, 47.25, 49.72, 53.08, 55.51, 55.81, 57.38, 58.21, 66.66, 68.19, 69.23, 70.74, 81.69, 85.15. 114.33, 130.13, 130.56, 158.85, 161.12, 168.49, 169.81, 169.91, 170.81, 171.38, 171.69, 172.60, 173.34, 197.64, 205.19. ESI-MS *m/e* Calcd for C$_{58}$H$_{87}$N$_7$O$_{15}$ 1121.6. Found 1122.3 [M + H]$^+$.

[(5*R*)-7-[(1*R*)-1-Carbonyl-3-methylbutyl]-1-isobutyryl-6-oxo-1,7-diazaespiro[4.4]nonane$^{7-9}$]aplidine (4b). White amorphous solid (10 mg, 69%). HPLC [HyperPrep PEP 100 C$_{18}$ (A/B, 85:15), ϕ = 7 mL/min] t_R = 19.0 min. ^{1}H NMR (300 MHz, CDCl$_3$): δ 0.86−1.00 (m, 24H), 1.12 (d, 3H, J = 7 Hz), 1.18 (d, 3H, J = 7 Hz), 1.34 (t, 2H, J = 7 Hz), 0.90−1.30 (m, 7H), 1.56−2.25 (m, 16 H), 2.30−2.80 (m, 3H), 2.55 (s, 3H), 2.95−3.06 (m, 1H), 3.15−3.25 (m, 3 H), 3.65 (dd, 1H), 3.52−3.79 (m, 6H), 3.79 (s, 3H), 3.98−4.15 (m, 1H), 4.28 (dd, 1H, J = 7 and 10 Hz), 4.59 (m, 2H), 4.79−4.85 (m, 2H), 5.17 (d, 1H, J = 4 Hz), 5.40−5.44 (m, 1H), 6.84 (d, 2H, J = 8 Hz), 7.06 (d, 2H, J = 9 Hz), 7.24 (d, 1H, J = 11 Hz), 7.90 (d, 1H, J = 9 Hz), 8.56 (d, 1H, J = 5 Hz). ^{13}C NMR (75 MHz, CDCl$_3$): δ 11.50, 14.92, 15.22, 16.68, 16.95, 18.50, 18.59, 18.81, 20.94, 23.42, 23.80, 24.49, 24.68, 24.90, 25.11, 26.91, 27.98, 30.93, 31.30, 35.58, 33.88, 34.16, 35.85, 36.24, 38.64, 38.84, 39.71, 41.29, 47.01, 47.76, 49.42, 49.62, 52.66, 55.26, 55.73, 57.12, 58.21, 66.57, 67.40, 68.10, 70.79, 81.57, 114.07, 130.05, 130.31, 158.57, 168.12, 169.66, 170.08, 170.56, 171.13, 171.96, 172.37, 174.04, 175.41, 205.04. ESI-MS *m/e* Calcd for C$_{59}$H$_{91}$N$_7$O$_{14}$ 1121.6. Found 1122.8 [M + H]$^+$.

[(5*R*)-1-(*tert*-Butoxycarbonyl)-7-[(1*R*)-1-carbonyl-3-methylbutyl]-6-oxo-1,7-diazaespiro[4.4]nonane$^{7-9}$]aplidine (4c). White amorphous solid (11 mg, 73%). HPLC [HyperPrep PEP 100 C$_{18}$ (A/B, 85:15), ϕ = 7 mL/min] t_R = 30.0 min. ^{1}H NMR (300 MHz, CDCl$_3$): δ 0.85−0.97 (m, 24 H), 1.19−1.34 (m, 18 H), 1.48 (s, 9H), 1.50−2.20 (m, 6 H), 2.32−2.36 (m, 1H), 2.54

(s, 3H), 2.58−2.72 (m, 2H), 2.97−3.08 (m, 1H), 3.10−3.22 (m, 3H), 3.34 (dd, 1H, $J = 4$ and 14 Hz), 3.46−3.79 (m, 6H), 3.79 (s, 3 H), 4.03−4.12 (m, 2H), 4.28 (dd, 1H, $J = 7$ and 13.2 Hz), 4.57−4.63 (m, 2H), 4.79−4.88 (m, 2H), 5.15 (d, 1H, $J = 3$ Hz), 5.21−5.23 (m, 1H), 6.84 (d, 2 H, $J = 8$ Hz), 7.07 (d, 2H, $J = 9$ Hz), 7.28 (d, 1H, $J = 11$ Hz), 7.79 (d, 1H, $J = 7$ Hz), 7.82 (d, 1H, $J = 10$ Hz). ^{13}C NMR (75 MHz, CDCl$_3$): δ 11.7, 15.2, 15.3, 16.8, 17.2, 18.7, 18.8, 21.2, 23.6, 23.9, 24.1, 24.9, 25.1, 25.4, 27.0, 28.2, 28.7, 29.9, 31.6, 34.5, 33.8, 34.2, 36.2, 36.6, 38.76, 39.1, 39.8, 41.3, 47.3, 47.8, 49.6, 49.9, 52.7, 55.5, 56.3, 57.4, 58.2, 66.7, 66.9, 68.3, 70.5, 80.7, 81.9, 114.3, 130.2, 130.5, 168.1, 169.8, 170.2, 170.8, 171.4, 172.5, 175.0, 205.0. ESI-MS *m/e* Calcd for C$_{60}$H$_{93}$N$_7$O$_{15}$ 1151.7. Found 1152.4 [M + H]$^+$.

[Hiv²]-[(5*R*)-7-[(1*R*)-1-carbonyl-3-methylbutyl]-6-oxo-1-pyruvyl-1,7-diazaespiro[4.4]nonane$^{7−9}$]aplidine (5a). White amorphous solid (10 mg, 72%). HPLC [HyperPrep PEP 100 C$_{18}$ (A/B, 85:15), ϕ = 7 mL/min] t_R = 13.6 min. ^{1}H NMR (300 MHz, CDCl$_3$): δ 0.80−1.10 (m, 24H), 1.11−1.80 (m, 12H), 1.81−2.30 (m, 10H), 2.45 (m, 1H), 2.55 (s, 3H), 2.57 (s, 3H), 3.07−3.43 (m, 6H), 3.52−3.77 (m, 6H), 3.78 (s, 3H), 3.91 (m, 1H), 4.03 (m, 1H), 4.29 (m, 1H), 4.63 (m, 1H), 4.72 (m, 1H), 4.87 (m, 1H), 5.03 (d, 1H, $J = 4$ Hz), 5.45 (m, 1H), 6.84 (d, 2H, $J = 8$ Hz), 7.07 (d, 2H, $J = 8$), 7.29 (d, 1H, $J = 9$ Hz), 7.81 (d, 1H, $J = 9$ Hz), 7.87 (d, 1H, $J = 5$ Hz). ESI-MS *m/e* Calcd for C$_{55}$H$_{83}$N$_7$O$_{14}$ 1065.6. Found 1066.4 [M + H]$^+$.

[Hiv²]-[(5*R*)-7-[(1*R*)-1-carbonyl-3-methylbutyl]-1-isobutyryl-6-oxo-1,7-diaza-espiro[4.4]nonane$^{7−9}$]aplidine (5b). White amorphous solid (10 mg, 70%). HPLC [HyperPrep PEP 100 C$_{18}$ (A/B, 85:15), ϕ = 7 mL/min] t_R = 16.9 min. ^{1}H NMR (300 MHz, CDCl$_3$): δ 0.80−1.07 (m, 24H), 1.08−1.47 (m, 12H), 1.48−2.30 (m, 16H), 2.36 (m, 2H), 2.56 (s, 3H), 2.65 (m, 1H), 2.96 (m, 1H), 3.18 (m, 2H), 3.36 (m, 2H), 3.65 (m, 6H), 3.78 (s, 3H), 3.91 (m, 1H), 4.02 (m, 1H), 4.25 (m, 1H), 4.63 (m, 1H), 4.72 (m, 2H), 4.87 (m, 1H), 5.02 (d, 1H, $J = 5$ Hz), 5.45 (m, 1H), 6.84 (d, 2H, $J = 9$ Hz), 7.07 (d, 2H, $J = 9$ Hz), 7.27 (d, 1H, $J = 5$ Hz), 7.88 (d, 1H, $J = 10$ Hz), 8.32 (d, 1H, $J = 5$ Hz). ESI-MS *m/e* Calcd for C$_{56}$H$_{87}$N$_7$O$_{13}$ 1065.6. Found 1066.7 [M + H]$^+$.

[Hiv²]-[(5*R*)-1-(*tert*-butoxycarbonyl)-7-[(1*R*)-1-carbonyl-3-methylbutyl]-6-oxo-1,7-diazaespiro[4.4]nonane$^{7−9}$]aplidine (5c). White amorphous solid (10 mg, 70%). HPLC [HyperPrep PEP 100 C$_{18}$ (A/B, 85:15), ϕ = 7 mL/min] t_R = 28.1 min. ^{1}H NMR (300 MHz, CDCl$_3$): δ 0.80−1.07 (m, 24H), 1.08−1.67 (m, 12H), 1.48 (s, 9H), 1.68−2.30 (m, 10H), 2.41 (m, 1H), 2.55 (s, 3H), 2.68 (m, 1H), 2.94 (m, 1H), 3.07−3.40 (m, 4H), 3.42−3.72 (m, 6H), 3.78 (s, 3H), 3.90 (m, 1H), 4.01 (m, 1H), 4.29 (m, 1H), 4.63 (m, 1H), 4.77 (m, 1H), 4.87 (m, 1H), 5.02 (d, 1H, $J = 5$ Hz), 5.25 (m, 1H), 6.84 (d, 2H, $J = 8$ Hz), 7.07 (d, 2H, $J = 8$ Hz), 7.31 (d, 1H, $J = 10$ Hz), 7.50 (d, 1H, $J = 6$ Hz), 7.85 (d, 1H $J = 10$ Hz). ^{13}C NMR (75 MHz, CDCl$_3$): δ 12.07, 14.25, 17.12, 17.92, 19.15, 21.11, 21.18, 23.80, 24.00, 24.06, 24.86, 25.08, 25.15, 27.58, 28.21, 28.82, 30.33, 31.18, 33.78, 34.28, 35.77, 36.65, 39.07, 39.45, 39.86, 46.91, 48.14, 48.47, 52.62, 55.49, 57.13, 58.42, 66.36, 66.80, 69.14, 70.84, 79.19, 80.55, 114.27, 130.29, 130.59, 154.12, 158.81, 168.25, 169.84, 170.72, 170.80, 170.90, 171.25, 174.89. ESI-MS *m/e* Calcd for C$_{57}$H$_{89}$N$_7$O$_{14}$ 1095.6. Found 1096.9 [M + H]$^+$.

[Hiv²]-[(5*R*)-7-[(1*R*)-1-carboxy-3-methylbutyl]-1-(2-methylacryloyl)-6-oxo-1,7-diazaspiro[4.4]nonane$^{7−9}$]aplidine (5d). White amorphous solid (10 mg, 72%). HPLC [HyperPrep PEP 100 C$_{18}$ (A/B, 85:15), ϕ = 7 mL/min] t_R = 16.4 min. ^{1}H NMR (300 MHz, CDCl$_3$): δ 0.85−0.96 (m, 18H), 1.02−1.05 (m, 6H), 1.14−1.45 (m, 12H), 1.49−1.64 (m, 4H), 1.68−1.77 (m, 1H), 1.89−2.05 (m, 3H), 1.99 (s, 3H), 2.10−2.28 (m, 4H), 2.43 (dd, 1H, $J = 8$ and 17 Hz), 2.57 (s, 3H), 2.60−2.68 (m, 1H), 2.97 (bs, 1H), 3.13−3.40 (m, 4H), 3.54−3.77 (m, 5H), 3.79 (s, 3H), 3.89−4.07 (m, 2H), 4.27 (m, 1H), 4.64 (m, 1H), 4.73 (m, 1H), 4.88 (m, 1H), 5.03 (d, 1H, $J = 4$ Hz), 5.30 (d, 1H, $J = 20$ Hz), 5.30−5.39 (m, 1H), 6.84 (d, 2H, $J = 8$ Hz), 7.08 (d, 2H, $J = 8$ Hz), 7.29 (s, 1H), 7.88 (d, 1H, $J = 10$ Hz), 8.23 (d, 1H, $J = 7$ Hz). ESI-MS *m/e* Calcd for C$_{56}$H$_{85}$N$_7$O$_{13}$ 1063.6. Found 1065.3 [M + H]$^+$.

Nuclear Magnetic Resonance Spectroscopy. Solutions of 59 mM spiropseudodipeptide **6a** in CDCl$_3$, acetone-d_6, and DMSO-d_6 were used for NMR experiments. ^{1}H NMR spectra were recorded on Varian INOVA 300 and 400 MHz spectrometers, and the ^{13}C NMR spectra were recorded on a Varian INOVA 300 operating at 75 MHz. Degassed solutions of 12 mM aplidine spirolactam analogue **4a** in CDCl$_3$ and DMSO-d_6 were used for NMR experiments. In this case, the ^{1}H NMR spectra were recorded on a Varian INOVA 500 MHz spectrometer, while the ^{13}C NMR spectra were recorded on a Varian Mercury 400 spectrometer operating at 100 MHz. The mixing time for the 2D TOCSY experiments was 70 ms, while for the NOESY spectra mixing times of 500 and 750 ms were used. The data were collected in phase using the hypercomplex method, and the spectral width used was 5141 Hz in the two dimensions. Four accumulations and 256 increments were carried out in the TOCSY period, and 16 accumulations and 128 increments were carried out in the NOESY experiments. The spectra were processed on Sun Microsystems SunBlade 100 and Ultra5 computers, using Varian VNMR 6.1C software. NOE buildup curves were generated from five NOESY experiments in DMSO-d_6 (mixing times of 100, 150, 200, 300, and 400 ms), using the distance between the (Leu³) NH and (Thr⁶) α-H determined in the X-ray structure of didemnin B for calibration purposes.

FT-IR Study of the Spiropseudodipeptide 6a. FT-IR spectra were recorded on a Perkin-Elmer-Spectrum One FT-IR spectrometer with 4 cm^{-1} resolution, using a 0.5 mm NaCl cell. The spectra were obtained with 64 scans, using 1.4, 5, and 14 mM solutions in dry CHCl$_3$ at room temperature. Background spectra were recorded with the solvent. The spectra were processed using the Perkin-Elmer Spectrum for Windows V3.02 software.

Molecular Modeling Calculations on the Spiropseudodipeptide 12. All calculations were run on an SGI workstation (Fuel, RP14000, 500 MB RAM) under an Irix 6.5 operating system. The initial conformation of the spiropseudodipeptide **12** was built using the library of fragments available in the molecular modeling program package Insight II (version 2000.1, Biosym Technologies, San Diego, CA). Molecular mechanics calculations were carried out using the AMBER force field as implemented in the DISCOVER module. They were conducted under vacuum with a distant-dependent dielectric constant (4*r*) and a cutoff of 14 Å. The structures were heated to 1000 K, equilibrated during 10 ps, and slowly cooled to 300 K stepwise. In each step the temperature was lowered by 100 K and the system was allowed to remain at the new temperature for 100 ps. After cooling to 300 K, the obtained conformations were energy-refined using a conjugated gradient algorithm with a final gradient of 0.001 kcal/mol as the convergence criterion. The conformers were stored and used to start a new simulation at high temperature. This procedure produced samples of 300 energy-minimized conformations, which were compared with each other to eliminate those that were identical and those more than 2 kcal/mol above the global minimum. The protocol was run three times, employing different starting structures of the spiro derivative **12**. Finally, the resulting minima were fully optimized, using the semiempirical AM1 Hamiltonian^{54} as implemented in the MOPAC module of the Insight II program package.

Molecular Mechanics/Dynamics Simulations on the Aplidine Spirolactam Analogue 4a. Molecular mechanics/dynamics calculations were performed on Silicon Graphics 02 (MIPS R5000 processor) and Octane (MIPS R12000 processor) computers running IRIX 6.5, using the well-established CHARMM program package^{69} (versions 29b1 and 24b2, respectively) and the CHARMm 23.1 force field.^{60,62} The initial structure of the *trans*-pyruvyl-Pro^8 isomer for modeling studies was produced by the requisite editing of the reported X-ray crystal structure of didemnin B. Both the CHARMm all-atom and united-atom representations of the molecule were modeled, the latter having all polar hydrogens explicitly represented. Charges were assigned to the atoms using the method described by Gasteiger and Marsili,^{70} and their suitability was confirmed by comparison with ESP charges derived from AM1-optimized small substructures for pyruvyl prolines, dimeth-

yltyrosine, and *N*-methyl amides employing MOPAC6. The Gaussian 94 program package using the Hartree−Fock 6-31G* basis set was used to check the adequacy of the force field parametrization for the pyruvamide function. After energy minimization the initial structures served as the starting point for *NVE* molecular mechanics/dynamics calculations at 300 K. These were performed without the introduction of restraints, incorporating both implicit ($\epsilon = 1$, 4.8, 45, and 80) and explicit solvent descriptions for H_2O and DMSO. For the latter cubic boxes of 30 Å side length and 1000 TIP3P water molecules[71] and of 31 Å side length and 216 DMSO molecules, respectively,[72] periodic boundary conditions were applied. After adequate heating and equilibration of the systems, evolution times were 10 ns for the all-atom implicit solvent simulations, 40 ns for all united-atom implicit solvent simulations, 4 ns for the DMSO united-atom explicit solvent simulation, and 2 ns for the united-atom H_2O explicit solvent simulation. Structures were saved periodically from each trajectory for further analyses. Trajectories were analyzed for bond distances, torsion angles, and hydrogen bonds by extracting the relevant information from the CHARMM output files.

Cytotoxicity Measurement. A colorimetric assay using the sulforhodamine B (SRB) reaction was adapted for a quantitative measurement of cell growth and viability, following the technique described by Skehan et al.[62] Cells (A549 and HT-29) were seeded in 96-well microtiter plates at 5×10^3 cells per well in aliquots of 195 µL of RPMI medium, and they were allowed to attach to the plate surface by growing in a drug-free medium for 18 h. Afterward, samples were added in aliquots of 5 µL [dissolved in (3:7) DMSO/H_2O]. After 48−72 h of exposure, cells were fixed by adding 50 µL of cold 50% (w/v) trichloroacetic acid and incubating at 4 °C for 60 min. Then the plates were washed with deionized H_2O and dried. A 100 µL solution of SRB (0.4% w/v in 1% acetic acid) was added to each microtiter well, and these were incubated at room temperature for 10 min. Unbound SRB was removed by washing with 1% acetic acid, the plates were air-dried, and the bound stain was solubilized with Tris buffer. Optical densities were read on an automated spectrophotometer plate reader at a single wavelength of 490 nm. Data analysis was automatically generated by the high-throughput screening laboratory information management system.

Supporting Information Available: Tables of ^{1}H and ^{13}C NMR chemical shifts for the spirolactam aplidine analogue **4a**, proton−proton distance measurements from the NOE buildup curves, calculated interatomic distances, torsion angles, and hydrogen bonding patterns for **4a**, and combustion analysis data. This material is available free of charge via the Internet at http://pubs.acs.org.

Note Added after ASAP Posting. This manuscript was released ASAP on 9/30/2004 with an author missing from the byline. The correct version was posted on 10/8/2004.

References

(1) Rinehart, K. L. Antitumor Compounds from Tunicates. *Med. Res. Rev.* **2000**, *20*, 1−27.

(2) Vera, M. D.; Joullié, M. M. Natural Products as Probes of Cell Biology: 20 Years of Didemnin Research. *Med. Res. Rev.* **2002**, *22*, 102−145.

(3) Caufield, C. E.; Musser, J. H. Chapter 21. Macrocyclic Immunomodulators. *Annu. Rep. Med. Chem.* **1989**, *25*, 195−204.

(4) Rinehart, K. L., Jr.; Gloer, J. B.; Hughes, R. G., Jr.; Renis, H. E.; McGovren, J. P.; Swynenberg, E. B.; Stringfellow, D. A.; Kuentzel, S. L.; Li, L. H. Didemnins: Antiviral and Antitumor Depsipeptides from a Caribbean Tunicate. *Science* **1981**, *212*, 933−935.

(5) Rinehart, K. L.; Lithgow-Bertelloni, A. M. Dehydrodidemnin B. WO 9104985, 1991.

(6) Raymond, E.; Paz-Ares, L.; Izquierdo, M.; Belanger, K.; Maroun, J.; Bowman, A.; Anthoney, A.; Jodrell, D.; Armand, J.-P.; Cortes-Funes, H.; Germa-Lluch, J.; Twelves, C.; Celli, N.; Guzman, C.; Jimeno J. Phase I Trials with Aplidine, a New Marine Derived Anticancer Compound. *Eur. J. Can.* **2001**, *37* (Suppl. 6), S32.

(7) Raymond, E.; Ady-Vago, N.; Ribrag, V.; Faivre, S.; Lecot, F.; Wright, T.; López-Lázaro, L.; Guzmán, C.; Jimeno, J.; Armand, J. P. Phase I and Pharmacokinetic Study of Aplidine, a Marine Derived Compound, Given as a 24h Infusion Every 2 Weeks in Patients (pts) with Advanced Solid Tumors and Non-Hodgkin Lymphoma (NHL). *Ann. Oncol.* **2000**, *11* (Suppl. 4), 134.

(8) Izquierdo, M. A.; Bowman, A.; Martínez, M.; Cicchella, B.; López-Lázaro, L.; Guzmán, C.; Germá, J.; Smyth, J. A Phase I Study of Aplidine (APL), a Marine Derived Compound, Given as a 1h Infusion Weekly × 3 in Advanced Solid Tumors and Non-Hodgkin Lymphoma Patients (pts.). *Ann. Oncol.* **2000**, *11* (Suppl. 4), 134.

(9) Maroun, J.; Belanger, K.; Seymour, L.; Soulieres, D.; Charpentier, D.; Goel, R.; Stewart, D.; Tomiak, E.; Jimeno, J.; Matthews, S. Phase I Study of Aplidine (APL) in a 1 Hour Daily Infusion × q 3 Weeks in Patients (pts) with Solid Tumors and Low and Intermediate Grade Non Hodgkins Lymphomas: A National Cancer Institute of Canada−Clinical Trials Group (NCIC−CTG) Study. *Ann. Oncol.* **2000**, *11* (Suppl. 4), 134.

(10) Urdiales, J. L.; Morata, P.; Nuñez De Castro, I.; Sánchez-Jiménez, F. Antiproliferative Effect of Dehydrodidemnin B (DDB), a Depsipeptide Isolated from Mediterranean Tunicates. *Cancer Lett.* **1996**, *102*, 31−37.

(11) Lobo, C.; García-Pozo, S. G.; Nuñez de Castro, I.; Alonso, F. J. Effect of Dehydrodidemnin B on Human Colon Carcinoma Cell Lines. *Anticancer Res.* **1997**, *17*, 333−336.

(12) Gomez-Fabre, P. M.; de Pedro, E.; Medina, M. A.; Nuñez de Castro, I.; Marquez, J. Polyamine Contents of Human Breast Cancer Cells Treated with the Cytotoxic Agents Chlorpheniramine and Dehydrodidemnin B. *Cancer Lett.* **1997**, *113*, 141−144.

(13) Erba, E.; Bassano, L.; Di Liberti, G.; Muradore, I.; Chiorino, G.; Ubezio, P.; Vignati, S.; Codegoni, A.; Desiderio, M. A.; Faircloth, G.; Jimeno, J.; D'Incalci, M. Cell Cycle Phase Perturbations and Apoptosis in Tumour Cells Induced by Aplidine. *Br. J. Cancer* **2002**, *86*, 1510−1517.

(14) Broggini, M.; Marchini, S. V.; Galliera, E.; Borsotti, P.; Taraboletti, G.; Erba, E.; Sironi, M.; Jimeno, J.; Faircloth, G. T.; Giavazzi, R.; D'Incalci, M. Aplidine, a New Anticancer Agent of Marine Origin, Inhibits Vascular Endothelial Growth Factor (VEGF) Secretion and Blocks VEGF−VEGFR-1 (flt-1) Autocrine Loop in Human Leukemia Cells MOLT-4. *Leukemia* **2003**, *17*, 52−59.

(15) Gajate, C.; An, F.; Mollinedo, F. Rapid and Selective Apoptosis in Human Leukemic Cells Induced by Aplidine through a Fas/CD95- and Mitochondrial-Mediated Mechanism. *Clin. Cancer Res.* **2003**, *9*, 1535−1545.

(16) Cuadrado, A.; García-Fernández, L. F.; González, L.; Suarez, Y.; Losada, A.; Alcaide, V.; Martínez, T.; Fernández-Sousa, J. M.; Sánchez-Puelles, J. M.; Muñoz, A. Aplidin Induces Apoptosis in Human Cancer Cells via Glutathione Depletion and Sustained Activation of the Epidermal Growth Factor Receptor, Src, JNK, and p38 MAPK. *J. Biol. Chem.* **2003**, *278*, 241−250.

(17) Sakai, R.; Stroh, J. G.; Sullins, D. W.; Rinehart, K. L. Seven New Didemnins from the Marine Tunicate *Trididemnum solidum*. *J. Am. Chem. Soc.* **1995**, *117*, 3734−3748.

(18) Sakai, R.; Rinehart, K. L.; Kishore, V.; Kundu, B.; Faircloth, G.; Gloer, J. B.; Carney, J. R.; Namikoshi, M.; Sun, F.; Hughes, R. G., Jr.; García-Gravalos, D.; de Quesada, T. G.; Wilson, G. R.; Heid, R. M. Structure−Activity Relationships of the Didemnins. *J. Med. Chem.* **1996**, *39*, 2819−2834.

(19) Schmidt, U.; Griesser, H.; Haas, G.; Kroner, M.; Riedl, B.; Schumacher, A.; Sutoris, F.; Haupt, A.; Emling, F. Synthesis and Cytostatic Activities of Didemnin Derivatives. *J. Pept. Res.* **1999**, *54*, 146−161.

(20) Vervoot, H.; Fenical, W.; Epifanio, R. A. Tamandarins A and B: New Cytotoxic Depsipeptides from a Brazilian Ascidian of the Family Didemnidae. *J. Org. Chem.* **2000**, *65*, 782−792.

(21) Liang, B.; Richard, D. J.; Portonovo, P. S.; Joullié, M. M. Total Syntheses and Biological Investigations of Tamandarins A and B and Tamandarin A Analogs. *J. Am. Chem. Soc.* **2001**, *123*, 4469−4474.

(22) Mayer, S. C.; Carroll, P. J.; Joullié, M. M. The Cyclic Depsipeptide Backbone of the Didemnins. *Acta Crystallogr.* **1995**, *C51*, 1609−1614.

(23) Jouin, P.; Poncet, J.; Dufour, M.-N.; Aumelas, A.; Pantaloni, A.; Cros, S.; François, G. Antineoplastic Activity of Didemnin Congeners: Nordidemnin and Modified Chain Analogues. *J. Med. Chem.* **1991**, *34*, 486-491.

(24) Hossain, M. B.; van der Helm, D.; Antel, J.; Sheldrick, G. M.; Sanduja, S. K.; Weinheimer, A. J. Crystal and Molecular Structure of Didemnin B, an Antiviral and Cytotoxic Depsipeptide. *Proc. Natl. Acad. Sci. U.S.A.* **1988**, *85*, 4118−4122.

(25) Kessler, H.; Will, M.; Antel, J.; Beck, H.; Sheldrick, G. M. Conformational Analysis of Didemnins. A Multidisciplinary Approach by Means of X-ray, NMR, Molecular Dynamics, and Molecular Mechanics Techniques. *Helv. Chim. Acta* **1989**, *72*, 530−555.

(26) Searle, M. S.; Hall, J. G.; Kyratzis, I.; Wakelin, L. P. G. Didemnin B. Conformation and Dynamics of an Antitumour and Antiviral Depsipeptide Studied in Solution by ¹H and ¹³C n.m.r. Spectroscopy. *Int. J. Pept. Protein Res*. **1989**, *34*, 445−454.

(27) Cardenas, F.; Thormann, M.; Feliz, M.; Caba, J. M.; Lloyd-Williams, P.; Giralt, E. Conformational Analysis of Dehydrodidemnin B (Aplidine) by NMR Spectroscopy and Molecular Mechanics/Dynamics Calculations. *J. Org. Chem.* **2001**, *66*, 4580−4584.

(28) Cardenas, F.; Caba, J. M.; Feliz, M.; Lloyd-Williams, P.; Giralt, E. Analysis of Conformational Equilibria in Aplidine Using Selective Excitation 2D NMR Spectroscopy and Molecular Mechanics/Dynamics Calculations. *J. Org. Chem.* **2003**, *68*, 9554−9562.

(29) Shen, G. G.; Zukoski, C. F.; Montgomery, D. W. A Specific Binding Site in Nb2 Node Lymphoma Cells Mediates the Effects of Didemnin B, an Immunosuppressive Cyclic Peptide. *Int. J. Immunopharmacol.* **1992**, *14*, 63−73.

(30) Mayer, S. C.; Ramanjulu, M.; Vera, M. D.; Pfizenmayer, A.; Joullié, M. M. Synthesis of New Didemnin B Analogs for Investigations of Structure/Biological Activity Relationships. *J. Org. Chem.* **1994**, *59*, 5192−5205.

(31) Genin, J. M.; Ojala, W. H.; Gleason, W. B.; Johnson, R. L. Synthesis and Crystal Structure of a Peptidomimetic Containing the (*R*)-4.4-Spiro Lactam Type II *β*-Turn Mimic. *J. Org. Chem*. **1993**, *58*, 2334−2337.

(32) Rodríguez, I.; Polanco, C.; Cuevas, F.; Méndez, P.; Cuevas, C.; Gallego, P.; Munt, S.; Manzanares, I.; García-López, M. T.; Gutiérrez, M.; Herranz, R. Synthetic Methods for Aplidine and New Antitumoral Derivatives, Methods of Making and Using them. EP 01945484.2-2404, 2001.

(33) Jou, G.; González, I.; Albericio, F.; Lloyd-Williams, P.; Giralt, E. Total Synthesis of Dehidrodidemnin B. Use of Uronium and Phosphonium Salt Coupling Reagents in Peptide Synthesis in Solution. *J. Org. Chem*. **1997**, 62, 354−366.

(34) Ottenheijm, H. C. J.; De Man, J. H. M. Syntheses of α-Keto Acid Chlorides. *Synthesis* **1975**, 163−164.

(35) Khalil, E. M.; Subasinghe, N. L.; Johnson, R. L. An Efficient and High Yield Method for the *N-tert*-Butoxycarbonyl Protection of Sterically Hindered Amino Acids. *Tetrahedron Lett.* **1996**, *37*, 3441−3444.

(36) Delaney, N. G.; Madison, V. Novel Conformational Distributions of Methylproline Peptides. *J. Am. Chem. Soc*. **1982**, *104*, 6635−6641.

(37) Beausoleil, E.; Lubell, W. D. Steric Effects on the Amide Isomer Equilibrium of Prolyl Peptides. Synthesis and Conformational Analysis of *N*-Acetyl-5-*tert*-butylproline *N′*-Methylamides. *J. Am. Chem. Soc.* **1996**, *118*, 12902−12908.

(38) Lee, Y.-C.; Jackson, P. L.; Jablonsky, M. J.; Muccio, D. D.; Pfister, R. R.; Haddox, J. L.; Sommers, C. I.; Anantharamaiah, G. M.; Chaddha, M. NMR Conformational Analysis of *cis* and *trans* Proline Isomers in the Neutrophil Chemoattractant, *N*-Acetyl-Proline-Glycine-Proline. *Biopolymers* **2001**, *58*, 548−561.

(39) Chernovitz, A. C.; Freedman, T. B.; Nafie, L. A. Vibrational CD Studies of the Solution Conformation of *N*-Urethanyl-L-Amino Acid Derivatives. *Biopolymers* **1987**, *26*, 1879−1900.

(40) Dumy, P.; Keller, M.; Ryan, D. E.; Rohwedder, B.; Wöhr, T.; Mutter, M. Pseudo-Prolines as a Molecular Hinge: Reversible Induction of *cis* Amide Bonds into Peptide Backbones. *J. Am. Chem. Soc.* **1997**, *119*, 918−925.

(41) Madison, V.; Kopple, K. D. Solvent-Dependent Conformational Distributions of Some Dipeptides. *J. Am. Chem. Soc.* **1980**, *102*, 4855−4863.

(42) Montelione, G. T.; Hughes, P.; Clardy, J.; Scheraga, H. A. Conformational Properties of 2,4-Methanoproline (2-Carboxy-2,4-methanoproline) in Peptides: Determination of Preferred Peptide Bond Conformation in Aqueous Solution by Proton Overhauser Measurements. *J. Am. Chem. Soc.* **1986**, *108*, 6765−6773.

(43) Magaard, V. W.; Sanchez, R. M.; Bean, J. W.; Moore, M. L. A Convenient Synthesis of the Conformationally Constrained Amino Acid 5,5-Dimehtylproline. *Tetrahedron Lett.* **1993**, *34*, 381−384.

(44) Halab, L.; Lubell, W. D. Effect of Sequence on Peptide Geometry in 5-*tert*-Butylprolyl Type VI *β*-Turn Mimics. *J. Am. Chem. Soc.* **2002**, *124*, 2474−2484.

(45) Kessler, H. Conformation and Biological Activity of Cyclic Peptides. *Angew. Chem., Int. Ed. Engl.* **1982**, *21*, 512−523.

(46) Belvisi, L.; Gennari, C.; Mielgo, A.; Potenza, D.; Scolastico, C. Conformational Preferences of Peptides Containing Reverse-Turn Mimetic Bicyclic Lactams: Inverse *γ*-Turns versus Type-II′ *β*-Turns—Insights into *β*-Hairpin Stability. *Eur. J. Org. Chem.* **1999**, 389−400.

(47) Alonso, E.; López-Ortiz, F.; del Pozo, C.; Peralta, E.; Macías, A.; González, J. Spiro *β*-Lactams as *β*-Turn Mimetics. Design, Synthesis, and NMR Conformational Analisis. *J. Org. Chem.* **2001**, *66*, 6333−6338.

(48) Boussard, G.; Marraud, M. *β*-Turns in Model Dipeptides. An Infrared Quantitative Analysis with NMR Correlation. *J. Am. Chem. Soc*. **1985**, *107*, 1825−1828.

(49) Gallo, E. A.; Gellman, S. H. Hydrogen-Bond-Mediated Folding in Depsipeptide Models of *β*-Turns and α-Helical Turns. *J. Am. Chem. Soc*. **1993**, *115*, 9774−9788.

(50) Jones, I. G.; Jones, W.; North, M. Conformational Analysis of Peptides and Pseudopeptides Incorporating an *endo*-(2*S*,3*R*)-Norborn-5-ene Residue as a Turn Inducer. *J. Org. Chem*. **1998**, *63*, 1505−1513.

(51) Luppi, G.; Lanci, D.; Trigari, V.; Garavelli, M.; Garelli, A.; Tomasini, C. Development and Conformational Analysis of a Pseudoproline-Containing Turn Mimic. *J. Org. Chem*. **2003**, *68*, 1982−1993.

(52) Weiner, S. J.; Kollman, P. A.; Case, D. A.; Singh, U. C.; Ghio, C.; Alagona, G.; Profeta, S., Jr.; Weiner, P. K. A New Force Field for Molecular Mechanical Simulation of Nucleic Acids and Proteins. *J. Am. Chem. Soc*. **1984**, *106*, 765−784.

(53) Cornell, W. D.; Cieplak, P.; Bayly, C. I.; Gould, I. R.; Merz, K. M., Jr.; Ferguson, D. M.; Spellmeyer, D. C.; Fox, T.; Caldwell, J. W.; Kollman, P. A. A Second Generation Force Field for the Simulation of Proteins, Nucleic Acids and Organic Molecules. *J. Am. Chem. Soc*. **1995**, *117*, 5179−5197.

(54) Dewar, J. M.; Zoebisch, E. G.; Eamonn, F. H.; Stewart, J. J. P. AM1: A New General Purpose Quantum Mechanical Molecular Model. *J. Am. Chem. Soc.* **1985**, *107*, 3002−3909.

(55) Rose, G. D.; Gierasch, L. M.; Smith, J. A. Turns in Peptides and Proteins. *Adv. Protein Chem.* **1985**, *37*, 1−109.

(56) Wilmot, C. N.; Thorton, J. M. *β*-Turns and Their Distortions a Proposed New Nomenclature. *Protein Eng.* **1990**, *3*, 479−493.

(57) Chou, K.-C. Prediction of Tight Turns and Their Types in Proteins. *Anal. Biochem.* **2000**, *286*, 1−16.

(58) Perczel, A.; Hollósi, M.; Sándor, P.; Fasman, G. D. The Evaluation of Type I and Type II *β*-Turn Mixtures. *Int. J. Pept. Protein Res.* **1993**, *41*, 223−236.

(59) Neuhaus, D.; Williamson, M. P. *The Nuclear Overhauser Effect in Structural and Conformational Analysis*, 2nd ed.; John Wiley and Sons: New York, 2000.

(60) Momany, F. A.; Rone, R. Validation of the General Purpose QUANTA 3.2 CHARMm Force Field. *J. Comput. Chem.* **1992**, *13*, 888−900.

(61) Momany, F. A.; Rone, R.; Kunz, H.; Frey, R. F.; Newton, S. Q.; Schäfer, L. Geometry Optimization, Energetics and Solvation Studies on Four and Five-Membered Cyclic and Disulfide Bridged Peptides, Using the Programs QUANTA 3.3 and CHARMm 22. *J. Mol. Struct.: THEOCHEM* **1993**, *286*, 1−18.

(62) Skehan, P.; Storeng, R.; Scudiero, D.; Monks, A.; McMahon, J.; Vistica, D.; Warren, J. T.; Bokesch, H.; Kenney, S.; Boyd, M. R. New Colorimetric Cytotoxicity Assay for Anticancer-Drug Screening. *J. Natl. Cancer Inst.* **1990**, *82*, 1107−1112.

(63) Shen, G. K.; Zukoski, C. F.; Montgomery, D. W. A Specific Binding Site in Nb2 Node Lymphoma Cells Mediates the Effects of Didemnin B, an Immunosuppresive Cyclic Peptide. *Int. J. Immunopharmacol*. **1992**, *14*, 63−73.

(64) Fischer, G. Peptidyl-Prolyl *cis/trans* Isomerases and Their Effectors. *Angew. Chem., Int. Ed. Engl.* **1994**, *33*, 1415−1436.

(65) Schmid, F. X. Prolyl Isomerases. *Adv. Protein Chem.* **2002**, *59*, 243−282.

(66) Schiene-Fischer, C.; Yu, C. Receptor Accessory Folding Helper Enzymes: The Functional Role of Peptidyl Prolyl *cis/trans* Isomerases. *FEBS Lett.* **2001**, *495*, 1−6.

(67) Gothel, S. F.; Marahiel, M. A. Peptidyl-Prolyl cis−trans Isomerases, a Superfamily of Ubiquitous Folding Catalyst. *Cell. Mol. Life Sci*. **1999**, *55*, 423−36.

(68) Shaw, P. E. Peptidyl-Prolyl Isomerases: A New Twist to Transcription. *EMBO Rep*. **2002**, *3*, 521−526.

(69) Brooks, B. R.; Bruccoleri, R. E.; Olafson, B. D.; States, D. J.; Swaminathan, S.; Karplus, M. A Program for Macromolecular Energy, Minimization and Dynamics Calculations. *J. Comput. Chem.* **1983**, *4*, 187−217.

(70) Gasteiger, J.; Marsili, M. Iterative Partial Equalization of Orbital Electronegativity a Rapid Access to Atomic Charges. *Tetrahedron* **1980**, *36*, 3219−3288.

(71) Jorgensen, W. L.; Chandrasekhar, J.; Madura, J. D.; Impey, R. W.; Klein, M. L. Comparison of Simple Potential Functions for Simulating Liquid Water. *J. Chem. Phys.* **1983**, *79*, 926−935.

(72) Liu, H.; Mueller-Plathe, F.; van Gunsteren, W. F. A Force Field for Liquid Dimethyl Sulfoxide and Physical Properties of Liquid Dimethyl Sulfoxide Calculated Using Molecular Dynamics Simulation. *J. Am. Chem. Soc.* **1995**, *117*, 4363−4366.